STRUCTURE PROPERTY RELATIONSHIPS IN TRACK PAD RUBBER AS A FUNCTION OF BLENDING CONDITIONS.

by

DAVID ERNEST RODRIGUES

Thesis submitted to the Faculty of the

Virginia Polytechnic Institute and State University

in partial fulfillment of the requirements for the degree of

MASTER OF SCIENCE

in

MATERIALS ENGINEERING

APPROVED:

David W. Dwight, Chairman

Chester W. Spencer

Jack L. Lytton

17 May, 1987

Blacksburg, Virginia

STRUCTURE PROPERTY RELATIONSHIPS IN TRACK PAD RUBBER AS A FUNCTION OF BLENDING CONDITIONS.

by

DAVID ERNEST RODRIGUES

David W. Dwight, Chairman

MATERIALS ENGINEERING

(ABSTRACT)

Tank track pads have been known to degrade rapidly under adverse conditions, especially during cross country service where the average life has been estimated to be 500 miles. Several factors have been identified as being the cause for such low service life. One of these is the 'quality of dispersion' which plays an important role in the performance of any rubber compound. In order to evaluate the effect of the quality of dispersion on the service life of rubber compounds, a controlled blending experiment was carried out with a recipe modelled on a standard track pad formula. Mechanisms of failure produced by a bad dispersion have been identified. Two interesting observations were made, one of which was the formation of voids and the other was crack propagation along flow lines which are directly relatable to processing conditions.

Acknowledgements

The author wishes to acknowledge the constant support, guidance and advice from the committee chairperson Dr. David Dwight. Dr. Dwight's experience and insight played an important role in analysing some of the results.

The author also wishes to thank Dr. J. L. Lytton and Dr. C. W. Spencer for agreeing to be on his committee and for their support.

The author wishes to thank , for his encouragement, patience and all the help rendered during my experiments.

of the Akron Rubber Development Labs deserves a special thankyou for his cooperation in preparing the rubber samples and for his advice.

The author wishes to thank for helping with the experimental work and also for his guidance.

Last but not least, the author wishes to thank and for their support.

Table of Contents

List of Illustrations

List of Tables

Chapter 1

1.0 INTRODUCTION:

The primary ingredients of rubber compounds are the base polymer, filler, oil and curatives. The objective of processing is to transform the compounding materials into useful products by three basic operations of mixing, preshaping and vulcanising. Filler used in most rubbers is carbon black. Carbon black is the generic term for a wide variety of finely divided carbonaceous pigments produced by the pyrolysis of hydrocarbon gases or oils. About 95% of all carbon black produced is used as reinforcing agent in rubber(1). Without carbon black reinforcement, automobile tires which last for 30,000 miles would last only 3,000 miles(2). In order to achieve maximum reinforcement the carbon black is to be very well dispersed. However the property which determines reinforcing capability is an important economic factor in the processing of rubber. This review aims to explain qualitatively the effect of different mixing conditions on the dispersion of carbon-black.

1.1.1 NATURE OF CARBON BLACK;

Carbon black consists of aggregates which are formed by fusion of particles in the flame(3). The carbon black particles formed in the flame exists as agglomerates. Each agglomerate consists of several aggregates held together by cohesive forces. The aggregate is the smallest carbon black

entity that can exist by itself. Carbon black agglomerates undergo breakdown during incorporation into rubber, generally amounting to one fracture per aggregate(4) so that the aggregates in rubber contain 50-70% of the original number of particles depending upon the grade of black and the extent of mixing.

The number of primary particles fused together to form each aggregate and the complexity of their three dimensional arrangement contribute to a property known as structure. The structure, or bulkiness, of the aggregates has a marked effect on their performance in rubber. It is important, therefore that both the particle size and the degree of structure be carefully controlled and monitored during the carbon black manufacturing process. Structure is measured by absorption of dibutyl-pthalate(DBP) up to the point where the dry, crumbly carbon black suddenly starts to cohere. From the DBP absorption (DBPA) the average bulkiness of the individual aggregates can be calculated by making suitable allowances for the volume of liquid between the aggregates at the end point(5).

Another property of carbon black that plays an important role in the processing as well the final properties of rubber is the "surface area". Surface area is commonly expressed in $m^{2/gm}$ and is expressed in terms of iodine number, which is the amount of iodine adsorbed per gram of black, under conditions developed such that the iodine number would be approximately equal to the surface area(5). Most rubber grades of carbon black range from 30 to $130 m^2/gm$ surface area.

The primary unit of carbon black-"the aggregate" is a colloidal form of elemental carbon. Within the aggregate of carbon black, the carbon atoms are arranged in graphitic (i.e. polymeric) layers. The layers are generally parallel to the surface, with the inner layers being generally concentric as shown in figure (1) (6). Carbon black, as produced, contains appreciable amounts of hydrogen, oxygen, and sulphur. The sulphur level depends upon the feed-stock used. The sulphur is present as a tightly bound heterocyclic substituent for carbon in the polymeric layers, and appears to have very little influence on rubber properties in most elastomer systems. Hydrogen is bonded to the surface and to defect carbon atoms, both at the surface and in the interior, and to surface oxygen atoms. Oxygen is present at the surface bonded to defect oxygen atoms(6). The following table shows the various constituents of carbon black.

	Channel gas	HAF Oil	MT (gas)
% Carbon	96.2	98	99.4
Oxygen	3.2	0.7-0.9	---
Hydrogen	0.6	0.20-0.35	0.35
Sulfur	0-0.1	0.5-1.7	0.01-0.04
Ash	0.04	0.5	0.04-0.13

Table 1. Chemical Composition of Carbon Blacks.

1.1.2 MIXING OF RUBBERS AND THE INCORPORATION OF CARBON-BLACK.

Rubber mixing is an energy intensive process and can be performed in several kinds of mixers, i. e. internal mixers, mill mixers or continuous mixers. The dispersion of ingredients in rubber mixing is achieved by a combination of shear and extensional flows which are imposed by specific mixing process. Mixing has a direct effect on the product properties by controlling the filler dispersion. At the beginning of the compounding step, the carbon black is completely segregated from the rubber matrix. At first the rubber is folded over large clumps of carbon black which then break into finely divided agglomerates dispersed into the bulk of the rubber, the "occluded rubber" particles. These are large compared to the size of individual aggregate particles and to the steady state size of aggregate domains. This inclusion step corresponds to the first power peak observed in a internal mixer as can be seen in figure (2). With continued shearing
the aggregates are pulled apart, the number of particles increases, the particle size decreases and the effective volume fraction decreases. Therefore all properties which depend on volume fraction will depend upon the amount of mixing.

Several models have been proposed for the mixing of rubber and the incorporation of carbon black during this process. The starting point for all models which describe this mixing process is that particle size reduction and dispersion are the result of counterbalancing rate processes of particle break up and dispersion(7). The simplest models describe the breakdown process as a first order process whose rate constant depends upon the mixing power applied to the mixture and the breaking energy of the particles or the discrete phase.

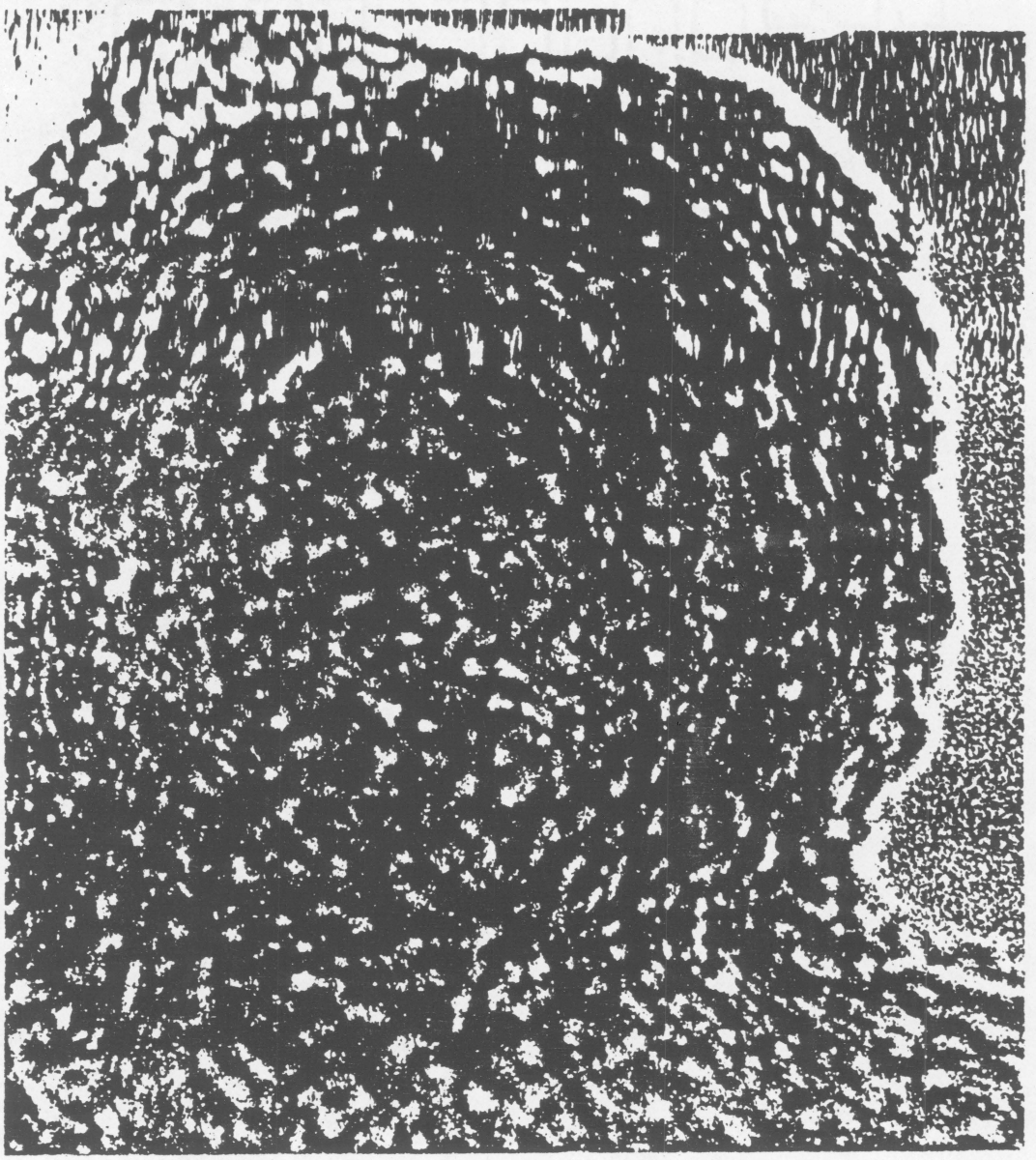

Figure 1. High resolution micrograph of carbon black particles.

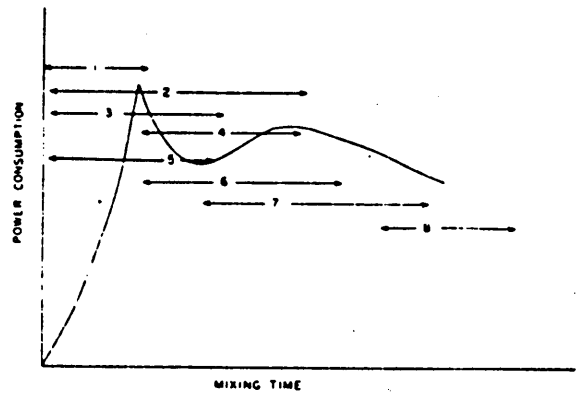

FIG. 2.—Material transformations processes in rubber processing: 1, fragment rubber, 2, distribute powders and liquids; 3, incorporate powders and liquids; 4, fuse fragments, 5, break down carbon black; 6, disperse black; 7, break down rubber and black-polymer interaction; and 8, shape compound.

Figure 2. Power curve involved in the mixing.

Tadmor(8) extended these analysis to pairs of interacting particles in a shear field. His model predicted that extensional flows had maximum forces which were twice as much as those involved in shear flows, deformation rate being the same. This difference in the forces causes a difference in the rate of carbon black dispersion, if particle fracture is the rate determining step. However agglomerates of many carbon-blacks are relatively weak because of cracks and many other imperfections in the structure, which lower their fracture strength as compared with that of a perfect agglomerate, so that kinematics control dispersion.

Theodorou(9) reviewed the extensive fluid mechanics literature on flow past solid and liquid particles. His model predicted higher forces for extensional flow than for shear flow and also that dispersion in extensional or shear flow is proportional to dispersion, while rate of dispersion is proportional to the rate of deformation.

Fedyukin et al (10) dispersed zinc oxide and vulcanising agents in either oil or water latex of PIP, or the additives used were in powder form. The latex dispersed additives had the smallest initial particles size and the powder had the largest the particles. The number of filler particles was largest for the latex while the particle size and distance between particles was smallest for this system. The reverse was true for the powder. The smaller latex prepared particles gave the most rapid network formation, the best distribution of crosslinks and the most elastic network. All these particles correlated with the particle size of the dispersed phase.

Many mechanical properties of a filled rubber are functions of the volume fractions of filler particles. The Guth-Gold equation predicts the stiffening effect of fillers on the modulus:

$$E_f = E_g(1 + 2.5\varphi + 14.1\varphi^2)$$

where E_f is the modulus of the filled rubber having an unfilled modulus E_g and having a volume fraction φ of the filler. When the volume fraction of the filler alone is used, the equation is inadequate but Medalia(4) introduced the concept of occluded rubber which states that the filler acts as if it had an effective volume φ_e:

$$\varphi_e = \varphi + \varphi_o$$

where φ_o is the occluded rubber volume fraction. The occluded rubber model asserts that a fraction of the rubber is effectively immobilised in the interstices of the secondary carbon-black particle which has a convoluted, open shape. The immobilised molecules tie several particles together which form agglomerates whose size is larger than the sum of the volumes of the particles alone. These agglomerates act as structural units in the matrix, and hence they are relevant particles to consider in theories of reinforcement. The effective volume depends upon the "structure" of the carbon black , which is a rough description of the architecture of secondary particles. The effective volume fraction can be calculated from the results of the standard DBPA test:

$$\varphi_e = \varphi(1 + 0.2139DBP)/1.46$$

Kraus extended these ideas to account for the effect of filler dispersion on cross-linking. He measured the stress for a fixed elongation using SBR, oil extended SBR and EDPM. The concentration of vulcanising agents as well as the filler concentration was varied. All of the data could be reduced to a single master curve as in the figure 3.

$\tau(\varepsilon) = (1 + k\varphi/1 - \varphi)^{-1} = \nu_o f(\varphi_e, t)$

where ν_o is the crosslink density of the unfilled rubber and k corrects for the influence of filler on crosslink reaction.

Cotton (11) described the incorporation process as the wetting of carbon black with rubber along with the squeezing out of the entrapped air. The progress of the dispersion was studied in terms of the power curve and divided into two stages. In the first stage of incorporation, the polymer encapsulates the black agglomerates. During the second stage the rubber is forced into the interstices in the aggregates; this corresponds with the second power peak. Rubber forced into these interstices is called bound rubber. As the rubber becomes incorporated into the black, the activity of the black increases. At a given carbon black activity, the amount of bound rubber increases with increasing molecular weight. The structure also plays an important role in the dispersion; higher the structure, lower the incorporation time.

MASTERBATCHES:

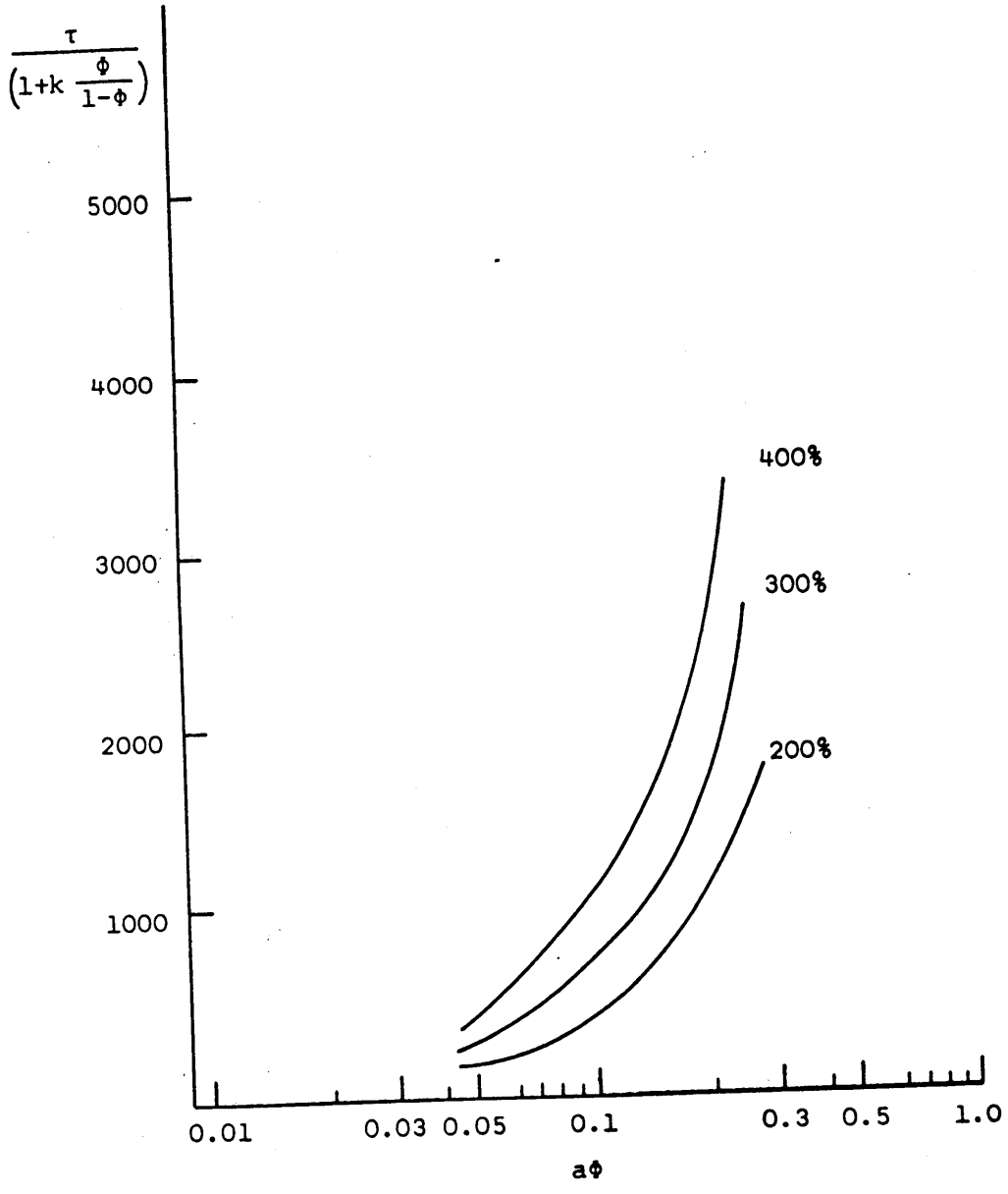

Figure 3. Master curve for filled rubber.

Rather than adding the ingredients directly to the main product the operator may choose to prepare a masterbatch. A masterbatch is a resin containing a high additive concentration which is diluted in the main matrix to yield the final product concentration. Masterbatches offer several advantages, the main one among them being cleanliness of operation. An important factor to be considered is that the use of a masterbatch requires an extra processing step, which increases processing costs. Hence the use of a masterbatch requires strong technical justification. Funt(12) has stated that the less rubber in the mix during particle fracture, the more efficient will be the use of energy. This may be a significant savings in favour of the use of masterbatches.

1.1.3 PHYSICAL TESTS:

Addition of carbon black to a rubber vulcanisate increases its strength and its abrasion resistance, but increases the heat build up in antivibration and shock absorption rubber applications. This heat build up occurs due to hysteresis which occurs whenever a rubber compound is subjected to cyclic stresses and strains. Hysteresis is that portion of stored strain energy that is not returned when stress is released and which is dissipated either as heat or plastic flow. Strain induced crystallisation in natural rubber is a major source of hysteresis. With amorphous rubbers attractive forces between polymer chains giving rise to intermolecular friction are a source of energy dissipation. Occluded rubber is highly restrained in its motion and hence does not contribute to hysteresis. Gehman, Woodford and Stambaugh studied the dynamic modulus of Hevea and GR-S gum in the frequency range 20 to 200 cycles. Stambaugh later reported that when hevea gum was subjected to compressional vibrations, amplitude effects were noted in the hysteresis of the filled compounds. Subsequent studies revealed that non-linearity of modulus with strain was most marked in compounds containing filler and also that the dynamic modulus at lower modulus was very sensitive to prior higher amplitude vibration.

The whole phenomonon has since been the subject of several investigations by Payne (22-25) who suggested that the decrease in modulus of filled blacks is due to the breakup of the three dimensional structure of carbon black. He states that the behavior of filler particles at low strains is different than at high strains. The in-phase shear G′ has a limiting value at low strains G_o and at

high strains G_∞ The difference can be correlated with the dispersion in the rubber vulcanisate. This difference $G'_o - G'_\infty$ decreases with improved dispersion. The phase angle δ which can directly be related to the hysteresis also decreases with improved mixing and dispersion; tensile properties are also improved. $G'_o - G'_\infty$ is a reliable index of dispersion in rubber filled composites (26). Payne (24) showed that hysteresis is low at low strains since factors such as G" and tan δ which are dependent upon energy dissipated have a low value); at moderate amplitudes the hysteresis is high because of the reformation and breaking up of interaggregate bonds and networks; at high strains there is low hysteresis because the network structure has already been destroyed and little energy needs to be expanded. However Medalia (3) has pointed out that when a specimen is oscillated about a midpoint, aggregates separated from each other at the ends of the cycle, may be brought into contact with each other during the middle of the cycle - a fact shown by electrical measurements. Thus it is reasonable to assume that interaggregate contacts contribute to hysteresis at high amplitudes of strain cycling. Hence modifications have to be made in the theory of hysteresis to explain such behavior.

Hysteresis is also produced due to stress softening. Stress softening can be defined as the phenomenon in which the amount of stress required to produce a given amount of elongation, decreases for each cycle in a fatigue/cyclic test. This produces considerable energy dissipation in the rubber compound. Theories have been proposed by Dannenberg(27) and Boonstra (28), which attempt to explain this phenomenon. Payne (26) claims that stress softening occurs in the gum phase of filler-loaded vulcanisates and not due to slippage of chains as claimed by others (27, 28).

R. W. Sambrook (16) conducted stress-strain experiments on different types of carbon-black reinforced rubber and used the "occluded volume" theory to explain results. He concluded that the relative stiffness $\frac{E_f}{E_g}$ decreases as the temperature increases and approaches a limiting value calculatable from filler volume fraction alone. He also stated that at low temperatures the low structure black provides the greatest tensile reinforcement.

Zvi Rigby stated that reinforcement produces some undesirable effects in the rubber compound. These are increased relaxation and creep rates, compression or tensile set, and hysteresis. He stated that a layer of polymer is adsorbed onto the carbon black surface; that the

process is one involving measurable rates; and the polymer may be desorbed provided sufficient energy is available; and this layer is fixed only in the direction perpendicular to the carbon black surface. This was confirmed by Wake who showed that similar behaviour was involved when C_4 and C_5 hydrocarbons were adsorbed onto the black.

Sambrook (16) attempted to explain the temperature sensitivity of carbon black reinforcement on the basis of carbon black morphology. He concluded that lowest structure blacks provide the greatest tensile reinforcement; however at higher temperatures the situation is reversed and higher structure blacks provide greater reinforcement. Carbon black activity along with base polymer morphology was also identified as being key variables when physical properties of rubber properties are considered. (In simplest terms carbon black activity is the affinity the filler has for its surrounding polymer matrix. The fact that higher structured blacks provide more reinforcement at higher temperatures raises the possibility that it is inter-aggregate separation that determines optimum filler level. By virtue of their greater bulkiness, and aggregate size, high structure fillers must of necessity be closer packed at given loading than lower structure materials.

Several authors have studied strength characteristics in terms of fracture mechanics, which treats fatigue and tensile failure as crack growth processes initiated from small flaws. This approach assumes that the energy necessary to cause a crack in a strained specimen to propagate at a certain rate (under a set of given conditions) is characteristic of the material and independent of the particular form of the specimen. When a stress is applied, crosslinks undergo scission and reformation. Oxygen and ozone also strongly influence crosslink scission. Thomas (19) devised an experiment in which a sharp line edge (e. g. blade) pulls a tongue of rubber from the fracture ridge producing crack growth at the base of the tongue. He was able to show quantitatively that the amount of rubber abraded was dependent on the amount of frictional force and the crack growth characteristics of the rubber. A. N. Gent et al. (20) and A. G. Thomas (21) conducted tearing experiments and concluded that fatigue and tensile failure are initiated from small naturally occuring flaws in the rubber. These probably arise from a combination of factors such as imperfect cutting of the sample edges, molding imperfections, dirt particles, and inhomogenities.

1.1.4 ELECTRICAL PROPERTIES:

It is well known that the degree of dispersion affects the electrical resistivity. This is because electric currents are carried by conducting paths formed by continuous chains of carbon black particles which form a more or less persistant structure in the rubber (32). This structure is deformed by the application of stresses and is reformed with time, the time for reformation decreasing with increasing temperature. The type of carbon black as well as its dispersion play an important role in electrical measurements. High structure carbon blacks give low resistivity value. Increased degree of dispersion will give higher values. Medalia (33) reported that at low loadings of carbon black the composite behaves like a dielectric because the polymer is non-conducting. As loading is increased a percolation threshold is reached where the conductivity begins to increase rapidly as a function of loading. The region of conductivity was called the percolation region. Thus Norman (34) has shown that d.c. or low frequency measurements of resistivity depend much upon contact resistance, and it is known that these properties change much during vulcanisation. The method of vulcanisation also affects the measured resistance. Boonstra et. al.(35) have concluded that an initial improvement in dispersion occurs when the resistivity passes through a minimum. This decrease in resistivity occurs due to the dispersion of the carbon black through the rubber which results in the formation of a stastical network. This shows that the resistivity is governed by the gap between the agglomerates. Cembrola (32) reported that once this minimum is exceeded there is a rapid increase in resistivity. With higher loadings there is a levelling of at higher mixing time. There is a continuous increase in resistivity at lower loadings even the 12 - 16 minute mixing time. This results from the continued randomisation of the carbon chain network to greater uniformity. Above a certain threshold volume loading, the carbon black network will be formed and result in a decrease in resistivity.

Sweitzer, Hess and Callan (36) reported considerable differences in dispersion associated with small changes in resistivity. Electrical measurements vary not only with dispersion, but are also a function of the curing system. Vulcanisation has been found to increase the resistivity of rubbers. A. C. measurements are sensitive to the presence of fillers, whether conducting or non-conducting.

Schneider et. al. (37) have reported that the resisitivity of conductive compounds does not change if measurements are made with AC or DC.

1.1.5 SURFACE ANALYSIS AND MICROSCOPY OF RUBBERS.

Wiegand (30) first attempted to measure carbon black dispersion using surface analytical techniques. He examined a torn surface using a hand lens; good dispersions gave smooth surface textures while bad dispersions gave rough surface textures. Stumpe and Railsback (31) of Phillips Petroleum developed a rating index wherein a set of standard photomicrographs were used to compare dispersions on a scale from 1 to 10. A 10 represented the best possible dispersion while a 1 indicated a very bad dispersion. In this method the cut surface of vulcanised rubber is examined under a light optical microscope at 30X and matched to a standard photomicrograph directly. Another method is to take a photograph of the section and compare with the standard. Hence in this method all dispersions are designated with a numerical rating. Microradiography and electron microscopy of sections of rubber compounds have been used extensively to study the dispersion of carbon black in rubber. Vegvari et. al. (29) in their overview of surface analytical methods used to characterise dispersion have mentioned that while some of these methods are superior to others in certain applications, they are generally inferior to optical microscopy for determining the level of carbon black agglomeration. Leigh-Dugmore (31) used thin frozen sections of vulcanised rubber cut by glass knives and viewed them under a light microscope with a micrometer ruled in the squares of the eyepiece. The total area covered by the black on the section is estimated from optical microscopy and 'percentage carbon black dispersion' is computed. Jansen and Kraus(14) conducted optical dispersion tests on carbon black dispersed in chloroform and butadiene rubber using the fact that the more finely divided the carbon black the more effectively it will screen out visible radiation. This method while being rapid also gives good correlation with results obtained from photomicrography. Optical extinction coefficients and, in particular, the ratio at two different wavelengths are used to estimate particle sizes in well dispersed blacks. The extinction coefficient is

E = -(1/lc)Ln(T/100) where T is the percent transmission, l is the thickness in metres, and c is the concentration in g/m^2 Dispersibility is the ratio of E at two preselected times.

$$Dispersibility = E(t_1)/E(t_2);\ t_2 > t_1$$

These methods give a good estimate of dispersion on a colloidal scale but are relatively insensitive to large undispersed agglomerates. A further observation made by the authors is that the modulus increases with mix time until a minimum degree of dispersion is obtained, whereupon it decreases with further mixing and improving dispersion. They also observed that as bulk density or structure increased there was an increase in the dispersability.

Ebell and Hemsley (15) used DFRL (dark field reflected light microscopy) to characterize rubber dispersions. They concluded that during the mixing there is first a short increase in the viscosity as the black is wetted by the polymer. As mixing increases there is a decrease in the viscosity due to filler deaggregation effects. However there is a critical mixing beyond which there is a decrease in the tear strength and the fatigue strength. This may be due to the excessive shear applied on the base polymer.

Sin-Shong LIN (16) performed ESCA and AUGER IMAGE ANALYSIS on track pad rubber that was subjected to UV degredation. Sliced samples were subjected to UV radiation in air for a period of one month in a small enclosure. The enclosure temperature was determined to be 105°C. Samples were then examined by ESCA followed by SAM. During SAM, ion beam was used to minimize extensive surface charging. ESCA data showed that oxidative degradation is linear with time. The Auger analysis also showed that the magnitude of oxygen signal increased roughly with the period of UV radiation. Auger image analysis showed that the additives of rubber formulation were not well dispersed. Particles or lumps 10um were observed. A large concentration of chlorine was detected, which the author attributed due to salt added during the fabrication of the rubber.

N. M. Mathew et al.(17) performed chemical and scanning electron microscopy on natural rubber vulcanisates that underwent fatigue failure. They studied a)effect of the vulcanising system b)effect of filler c) effect of antioxidant d) effect of test temperature. They concluded that addition of reinforcing black reduces the flexing resistance and also slightly decreases the crosslink density.

De Mattia tests showed that addition of HAF black makes mixes more brittle, and the mode of failure is changed to shear fracture, as compared with ductile failure in gum mixes. Addition of antioxidant changed the mode of failure from brittle to quasi-ductile. S. K. Chakraborty et al.(18) reported that fracture mechanisms depended upon the nature of the test as well the nature of the base polymer.

McDonald and Hess studied carbon black morphology in rubber using electron microscopy. An advantage of the EM technique is that measurements can be made in rubber samples as they exist in rubber compounds.

Chapter 2

2.0 EXPERIMENTAL MIXING

2.1.1 FORMULATION:

The formulation of a track pad formula would determine to a large extent the performance of the rubber. The ingredients in a rubber compound play an important role in the vulcanisation and the mixing. Numerous factors have to be taken into account while choosing the ingredients in order to obtain a suitable compound with good performance characteristics. Varying the type or quantity of carbon black, the percentage oil, or the use of predispersed curatives has a profound effect on the quality.

If smaller carbon black particles are used e. g. N110, then the abrasion resistance is improved, but it would be extremely difficult to disperse, and processing costs would increase tremendously. The larger size particles are easier to disperse but show less resistance to abrasion. Addition of large amounts of oil would make for easy processing, but because of the decrease in viscosity the reinforcing fillers and other curatives would not be homogeneously dispersed throughout the system. On the other hand too small a quantity of oil will give rise to processing problems because of too high a viscosity. Hence in order to obtain a rubber sample with good performance characteristics, it is obvious to that there must be a trade off in the oil added Vs. the type of black

used (especially for the high abrasion resistance blacks). This chapter consists of a section on formulation and one on the mixing.

All samples tested, consisted of the following ingredients in parts per hundred by weight.

INGREDIENTS	PARTS BY WEIGHT
STYRENE BUTADIENE RUBBER 1500	100
N234 CARBON BLACK	64
SUNDEX 8125 AROMATIC OIL	10
ZINC OXIDE	4
STEARIC ACID	1
AGERITE MA (ANTI OXIDANT)	2
SANTOFLEX (ANTI OZONANT)	1.3
OBTS (CURE ACCELERATOR)	1.7
SULFUR	1.9

Table 2. Ingredients used in the experiment.

However samples A-2, A-1, and B-1 utilized a masterbatch whose composition was as follows

INGREDIENTS	PARTS BY WEIGHT
SBR 1500	100
N234 CARBON BLACK	52
SUNDEX 8125 (HIGH AROMATIC OIL)	10

Table 3. Ingredients of masterbatch (SBR 3651).

According to ASTM classification the masterbatch recipe denoted above is classified as SBR 3651. This rubber, carbon black, oil master batch is made by stirring the carbon black and oil into the rubber latex (water emulsion as manufactured). The material is coagulated , washed, dried and baled. This intimate mixture brings the ingredients into close proximity for high shear mixing as will be discussed in the next section. This material required only 10 parts of the high abrasion resistant N234 carbon black and no additional oil to provide the necessary composition for a track pad formula. The absence of oil permits good dispersive conditions.

Preblended curatives were also used in samples A-2, A-1, and C-1. The predispersed curatives consisted of zinc oxide, sulfur and accelerator in minor level (20 to 30%) of the rubber.

2.1.2 MIXING

Proper mixing of elastomers is very important, for it is this process that determines the performance and the life of the rubber compound to a large extent, (the other important factor being the vulcanization system which determines the crosslink density and the nature and type of crosslinks). Mixing is an energy intensive process and it is the magnitude of shear forces that play an important role in the dispersion of the black. A Banbury was used to mix the ingredients for the rubber compounds used in these experiments. A Banbury is an internal mixer the schematic diagram of which is shown in figures (4) and (5).

A mixing operation in the Banbury, involves the rupture of the agglomerates, separation of closely packed particles after rupture, and the dispersion of the particles uniformly throughout the matrix. The first two processes are energy intensive, while the latter is primarily an extensive process. The internal mixer shown in figure (4) consists of a cylindrical chamber containing a pair of motor driven rotors. The rubber, filler and other solid components are introduced into the feed hopper, which leads into the mixing chamber. Liquid components are introduced directly into the chamber through an injection. The ram subjects the components to pressure, which helps the initial ingestion of the black into the rubber. After mixing, the discharge door is opened and the mixed rubber is removed and sent forward to the next processing operation. Both Banburies used in his work were manufactured by Farrel. Their specifications are as follows:

Farrel ID: large scale production unit, has total power of 200HP, total volume of 16000ml., a continuous range of speeds varying from 0 - 100 r. p. m. The ram diameter is 8 inches. Pressure applied by the ram is approximately 60psi. Farrel B, laboratory model, is of 25 HP and has a total volume of 1300ml. It has only 4 speeds and has ram diameter of 6 inches. Ram pressure is approximately 30psi during mixing. A maximum pressure of 100psi can be applied in both the Banburies, but this can be dangerous.

The mixing of the various batches was as follows:

Compound A-1 was a 25 pound batch consisting of SBR 3651 mixed with N234, zinc oxide, stearic acid and anti oxidants (all in at the start) at 40 r. p. m. in a Farrel ID Banbury. The temperature rise was from 200°F to 240°F. The mixing time was 1.75 minutes and no cooling water

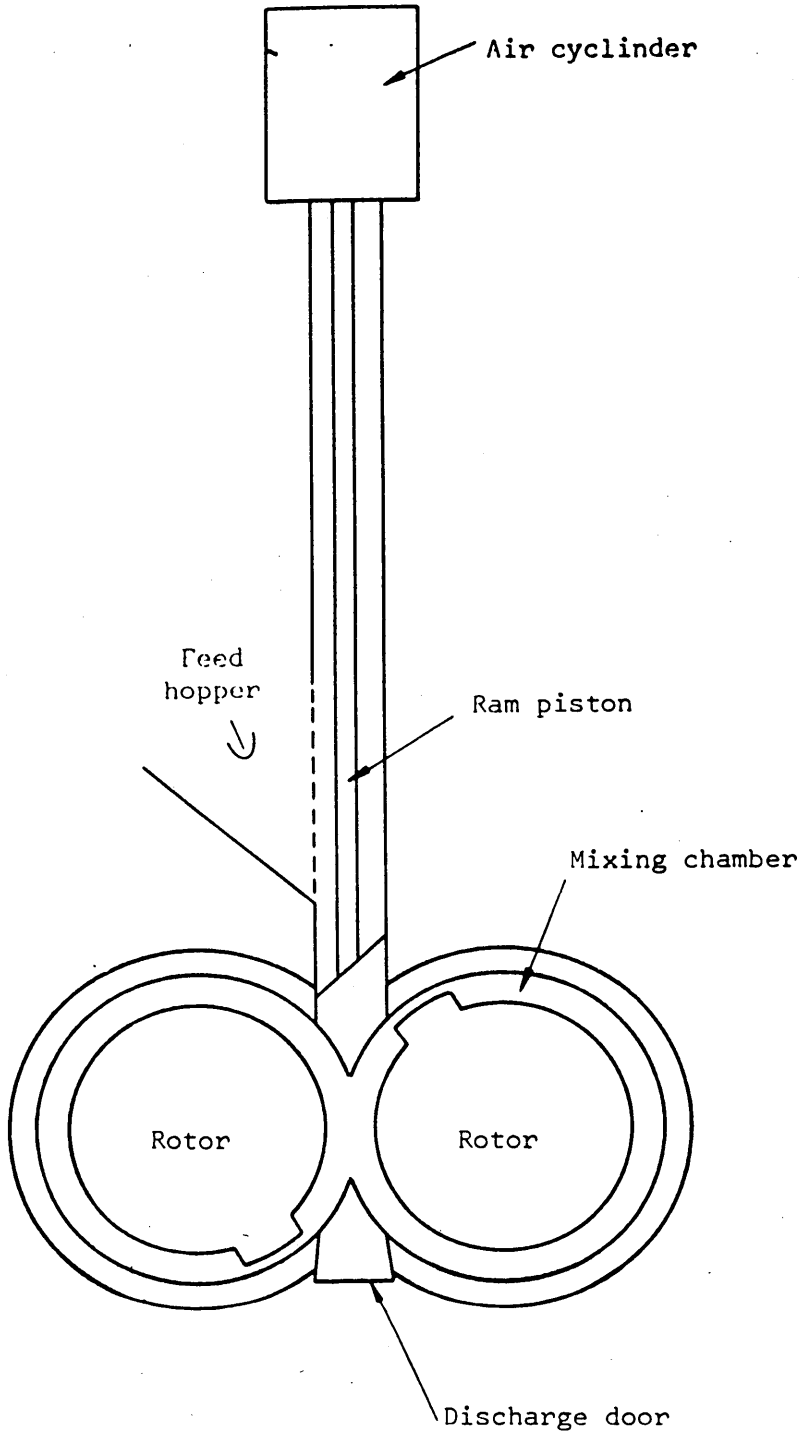

Figure 4. Schematic view of an internal mixer.

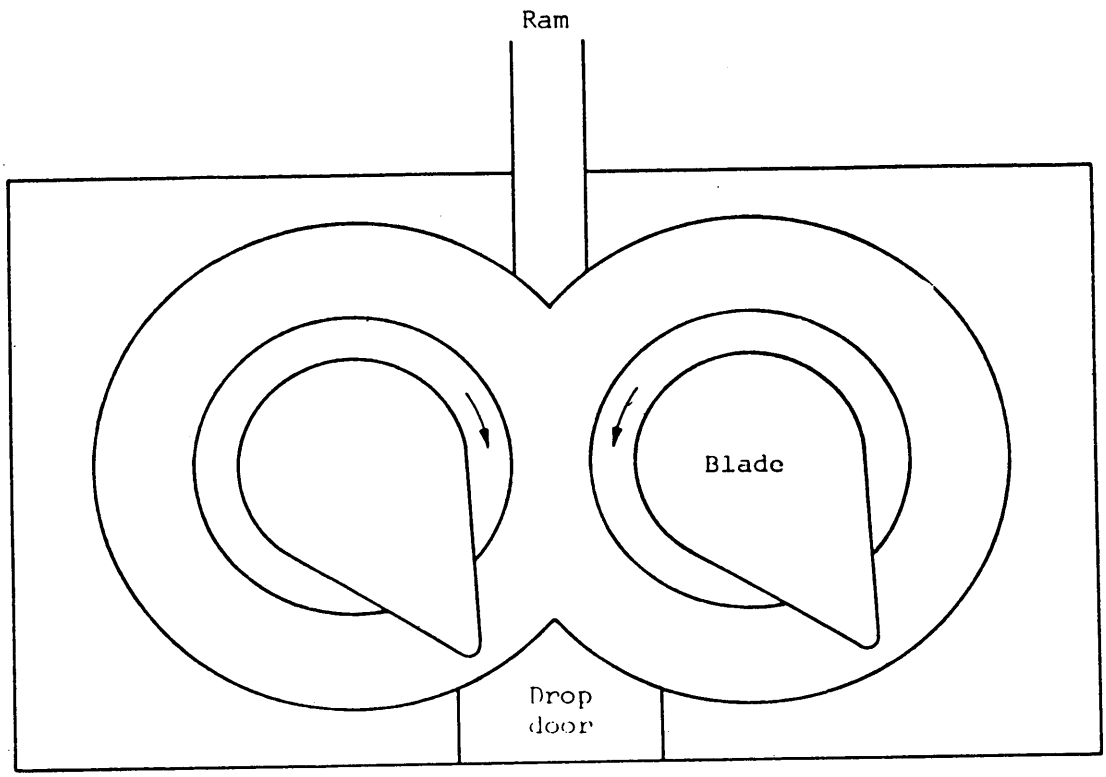

Figure 5. Mixing chamber cross-section.

was used. Sulphur and OBTS were added on a warm 130°F, 40 Inch mill set at 1/4″ open. Predispersed forms of zinc oxide, sulphur and OBTS were utilized in compound A-1.

Compound B-1 followed A-1 while the mixer was still warm and was the same as A-1 except that zinc oxide, sulfur and OBTS were added in a regular manner and not as a predispersed mixture.

Compounds C-1 and D-1 were mixed "upside down", utilizing SBR 1500, loose N234 black and "free" oil. "Upside down" dispersion means that the additives are added first, and the rubber was introduced last. This method is used where dispersion is not critical or other conditions (e. g. large amounts of oil) require it. In this case the curatives were added before the rubber too. The Banbury was speeded up to 50 r. p. m. for compound C-1 (mix time - 1.33 minutes) and to 60 r. p. m. for compound D-1 (mix time - 1.77 minutes). The batches followed B-1 in a warm Banbury (no cooling water was used) and were quickly end rolled eight times at 3/8″ open sheeted from a 40 inch mill at 130°F.

Compound D-1 contained a regular zinc oxide, sulfur and OBTS powder while C-1 contained the predispersed forms of the ingredients. Compound A-2 was produced from 1000 grams of compound A-1. The material was passed twenty times through an end roll mill at 150°F. To avoid affecting the dispersion quality, the compounds A-2, A-1, B-1, C-1, D-1 were cured without further milling except for specimens used in the flexometer tests since some milling is required to fit these into the cylindrical mould. Even here the milling forces were insufficient to remove the 'flow lines'.

To obtain poorer dispersion, new samples E-1, F-1 and G-1 were prepared. The same recipe for D-1 was used for these. However they were mixed in the smaller laboratory Banbury mixer at 77 r. p. m. To reduce shear, the rubber was masticated and warmed for increasing periods to reduce the viscosity, then the remaining ingredients were added for a 1.0 minute mix as follows: The mixer was stopped while the non-rubber ingredients were added. After 30 seconds the mixer was stopped for a ram scrape down. After another 30 seconds the Banbury was again stopped and opened for another batch discharge. These batches were passed through the 12″ lab mill at 130°F with the nip maintained at 1/4″ open. These batches were given minimum further milling only for the ASTM D 623 flexometer blowout tests.

Chapter 3

3.0 CHARACTERIZATION OF RUBBER

3.1.1 DESCRIPTION OF PHYSICAL TESTING MACHINES

3.1.1.1. GOODRICH FLEXOMETER

In this method, which uses the Goodrich flexometer, the specimen was subjected to a fixed compressive load through a lever system which has a high inertia, while simultaneously imposing on the specimen an additional high frequency cyclic compression of definite amplitude. Heat was generated during this cyclic deformation process. The change in temperature was measured by means of a thermocouple at the center of the lower anvil. It is possible to continuously measure the change in the height of the specimen during testing. This can be used to give an idea of the permanent set or stiffness of the specimen. Specimens may be tested by using a constant initial load stress or a constant initial compression strain. A diagram of the basic parts of the flexometer is shown in figure (6). The experiment was conducted as follows. The test piece was placed between anvils. The top anvil was connected to an adjustable eccentric driven between 800 to 1800 r. p. m. The load was applied by means of the lever resting on the knife edge. Weights were suspended on the lever at both ends, equidistant from the knife edge. The anvil could be raised or lowered from

the lever by means of the micrometer. The micrometer was used to maintain the bar in the horizontal during a test.

Before starting the test the bar was set horizontal. This was accomplished when the bottom anvil was lowered/raised so as to allow a metal piece 1 inch high to be inserted between anvils. The calibrated micrometer was set at zero and the pointer was set on a mark at the end of a lever bar to indicate the zero position. When the test piece was inserted and the load applied, the bar was again returned to zero position by turning the micrometer mechanism.

In our experiments the Goodrich Flexometer was used to study the heat build up in rubber samples subjected to cyclic fatigue under compressive loads. Samples of rubber from the blowout region were cryomicrosectioned and examined under TEM, to study differences in carbon black dispersion before and after flexing.

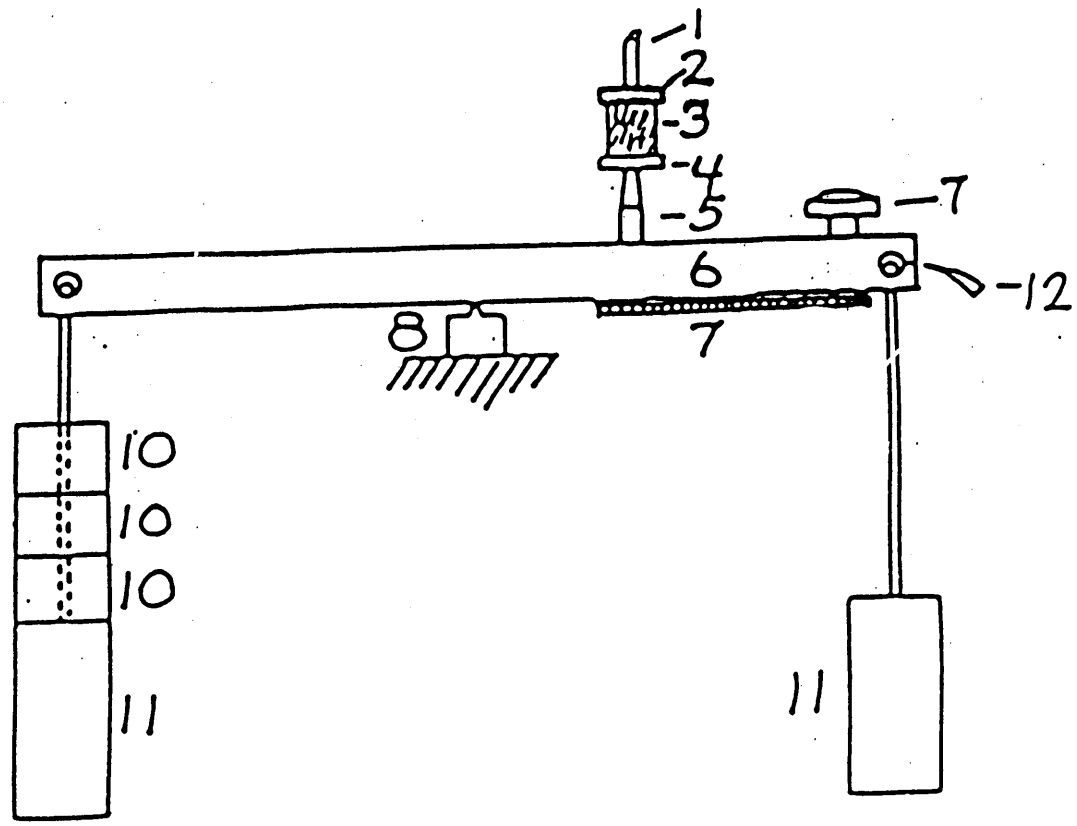

Figure 6. Goodrich Flexometer

3.1.1.2 DE MATTIA FLEX TEST:

This method was used to study the crack growth of vulcanized rubber when subjected to repeated bend flexing. In order to study the flexing fatigue of vulcanized products, a hole was pierced in the flex area. The piercing tool as well as the ASTM specifications for it are shown in figure (7). Figure (8) shows the test specimen as well as the die specifications. The machine consists of a head with a grip, which holds one end of the sample in a stationary position; a reciprocating grip holds the other end. The reciprocating end moves in the same plane as the center line between the two grips. The travel of the moving member is adjusted by means of a connecting rod and eccentric and is permitted a maximum travel of 100mm.

Test were conducted on molded specimens, conforming to the shape and dimensions given in ASTM D 813. The surface was free from all defects in the measured area. The circular groove was located midway between the grips. After the necessary adjustments were made, the test was conducted and the time recorded. At the end of varying time periods of operation, the number of flexing cycles was calculated by multiplying the observed time in minutes by the machine rate of 300 cpm. During the test the machine was stopped frequently and the crack length was measured as accurately as possible.

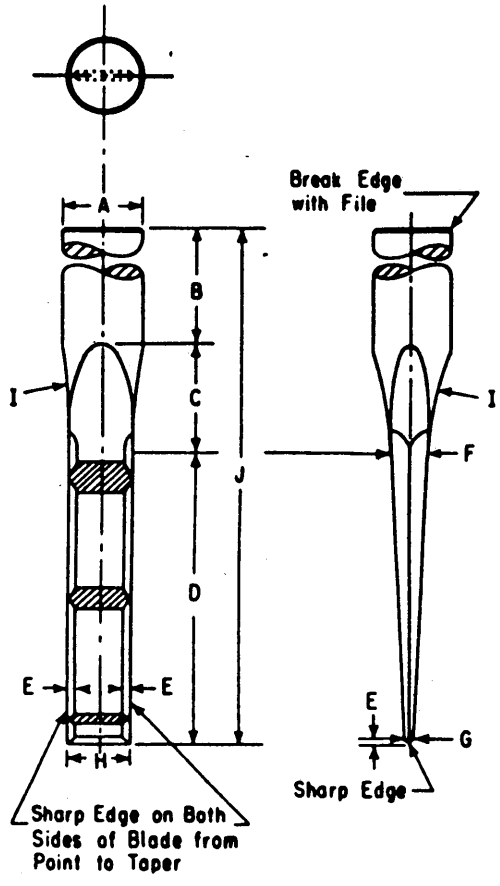

	mm		in.	
A	2.62		0.103	
B	44.5 ± 0.4		1.75 ± 0.015	
C	3.8 ± 0.4		0.150 ± 0.015	
D	10.3 ± 0.1		0.400 ± 0.005	
E	0.38 + 0.05	0.00	0.015 + 0.002	0.000
F	1.00 + 0.05	0.00	0.041 + 0.002	0.000
G	2.03 + 0.05	0.00	0.080 + 0.002	0.000
I	25 rad		1.0 rad	
J	58.42		2.300	

Figure 7. Piercing tool.

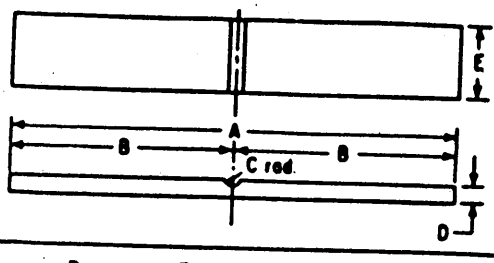

	A	B	C	D	E
mm	150	75	2.39 ± 0.03	6.35 ± 0.13	25
in.	6	3	0.094 ± 0.001	0.250 ± 0.005	1

FIG. 2 Test Specimen with Circular Groove

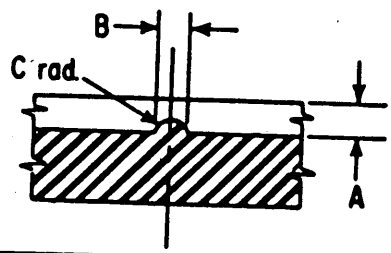

	A	B	C
mm.	6.45 ± 0.03	4.83 ± 0.03	2.39 ± 0.03
in.	0.254 ± 0.001	0.190 ± 0.001	0.094 ± 0.001

Figure 8. Test specimen and its die with specifications.

3.1.1.3 TENSILE TEST

Tension tests were made on a power driven machine equipped with a uniform rate of grip separation at 8.5 &PM. 0.8 mm/sec. It has two grips one of which is connected to a dynamometer. In order to prevent slipping of the specimen, gripping pressure increases as the tensile force increases. The dynamometer has a recording device for measuring applied forces to within &PM.2%. The tensile testing machine has a chamber for conducting tests at elevated and low temperatures. The specimens were mounted vertically in the chamber so that they may be suitably conditioned. The rapid gripping system in the chamber, provides for quick interchange of specimens so that there is no appreciable temperature change between tests. A diagram of the testing machine is shown below in figure (9).

Dumbell shaped specimens were used for these tests. The grain direction has an effect on the results and hence specimens should be cut with their grain direction parallel to the mill direction.

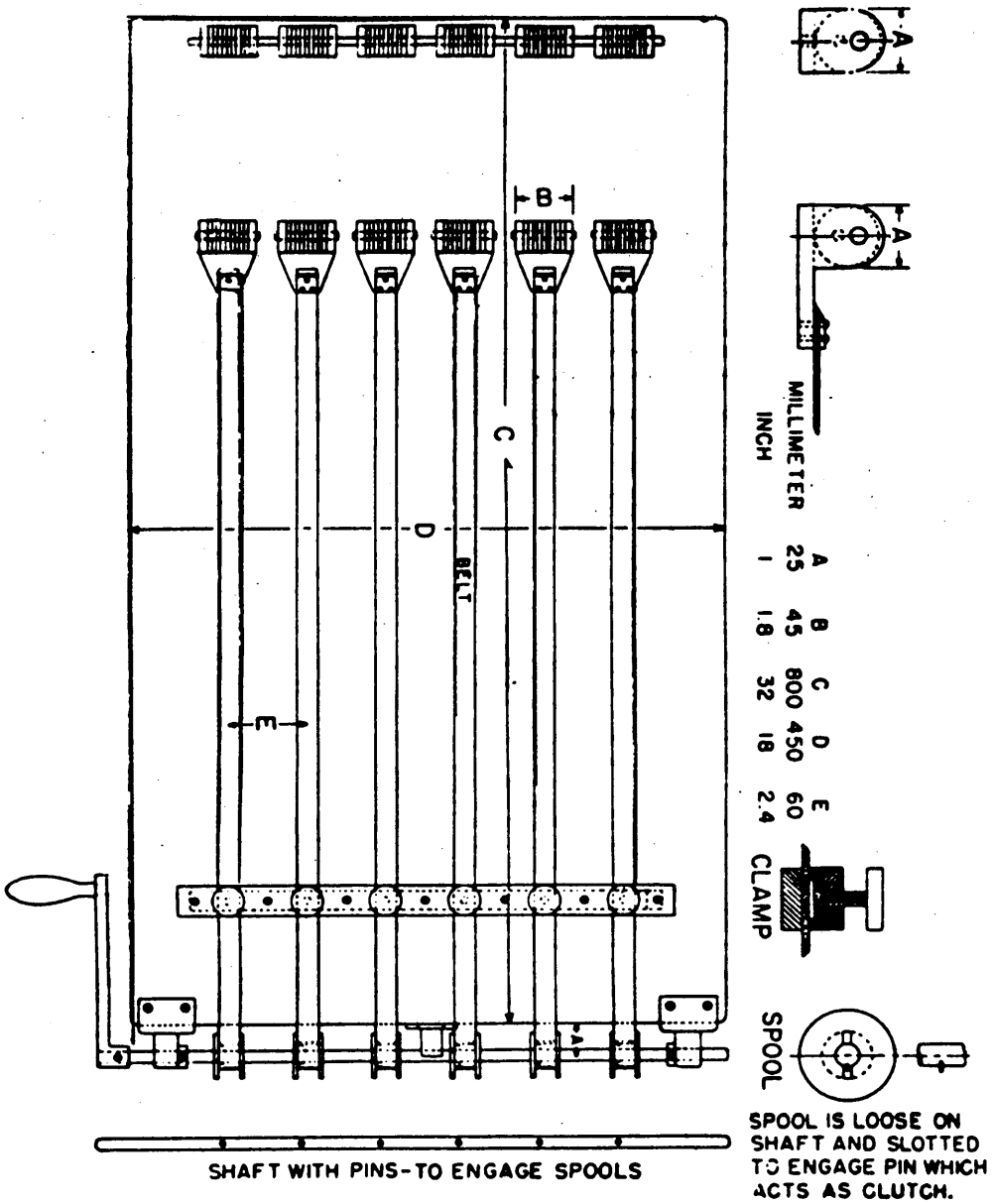

Figure 9. Tensile testing machine.

3.1.1.4 NICKED TEAR TEST (DIE B)

In many service applications rubber fails by the initiation and propagation of a special type of rupture called a tear. This test was used to determine the tear resistance of vulcanized rubber. The test specimens used were Die B type (shown in figure 10) and conformed to ASTM D 624 specifications. The testing apparatus was similar to that used in the tensile test ASTM Method D 412. The grips holding the ends of the specimen were pulled apart at 500 &PM. 50mm/min.

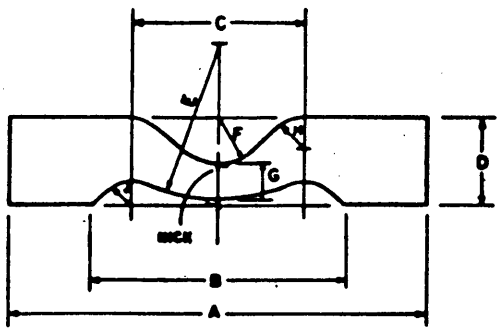

DIE B (ISO/34 CONFIGURATION)

Dimension	Millimetres		Inches	
	Value	Tolerance	Value	Tolerance
A	110	±0.50	4.3	±0.02
B	68	±0.50	2.7	±0.02
C	45	±0.05	1.8	±0.002
D	25	±0.05	1	±0.002
E	43	±0.05	1.7	±0.002
F	12.5	±0.05	0.5	±0.002
G	10.2	±0.05	0.4	±0.002
H	9	±0.05	0.375	±0.002
J	7.5	±0.05	0.3	±0.002
Nick[A]	0.5	±0.05	0.02	±0.002

[A] Nick to be cut in specimen with a razor.

Figure 10. Die B test specimen

3.1.1.5 PICO ABRADER:

Abrasion resistance of soft vulcanisates and other elastomeric compounds is usually determined using a Pico abrader. In this method tungsten carbide blades of predetermined sharpness and geometry were rubbed over the surface of rubber specimens in a rotary fashion under controlled conditions of load, time and speed. During the rubbing process a dust was spread over the specimen and at the interface between the knife and the specimen to help remove the abraded particles and also to prevent the blade from being coated with oil and resin.

The specimen was clamped on the turntable driven by a variable speed motor capable of rotating in both directions. The number of revolutions were counted by means of a pair of counters. The dust was sprinkled on the sample and the interface at a constant rate from dust feeder tubes. The force on the knives can be regulated by means of a box into which steel or lead pieces can be placed.

Five samples were prepared according the specifications in ASTM D 2228, section 6, and these were used for caliberating the abrader as well for comparing the performance of other samples. They were first buffed using a grinding wheel and then brushed to remove all loose rubber particles. The mass was determined before the samples were abraded. The rotational frequency was adjusted to 1 &PM.0.03 Hz by means of a rheostat. The force on the knives is 44 N. The samples were subjected to 80 revolutions i. e. 40 revolutions in each directions. The mass of the specimens were again determined after the abrasion had taken place.

3.1.1.6 MOONEY VISCOMETER:

This method utilises a shearing disc to determine the viscosity and vulcanising characteristics of rubbers and other elastomers. Viscosity values determined by this method depend upon the molecular structure and upon non-rubber constituents that may be present. Since rubber behaves as a non-Newtonian fluid, no simple relationship exists between the molecular mass and the viscosity. In this test, measured is the torque required to rotate a disc embedded in a rubber specimen placed in a rigid cavity (under given conditions of temperature and pressure) is slowly and continuously rotated in one direction. This instrument consists of a motor driven disc placed between two dies which form the die cavity. The dies are maintained under specific conditions of temperature and die closure force. Closure force is very important and hence it should be correct for a particular experiment. The temperature of the dies is measured by means of thermistors; it being almost impossible to measure the actual sample temperature. The viscometer was adjusted so that it reads zero, when there was no sample and reads 100 &PM. 0.05 J when a torque of 8.30 &PM. 0.02 J was applied to the rotor shaft. Therefore a torque of 0.083 J is equivalent to one Mooney unit. The set up for the Mooney viscometer is shown in the figure (11).

The viscometer was used to determine the change in viscosity with mixing. The temperature of the dies was maintained at 212°F and the large disc was used during the experiment. The torque indicator was adjusted to zero when the rotor was running in the unloaded condition. The hot rotor was then removed from the conditioned cavity and the test pieces were quickly inserted into the viscometer. The specimen was heated for one minute and then the motor was started. The viscosity was measured instantly i. e. as soon as the sample was introduced into the cavity. Measurements were also made at 1.5 minutes and at 4.0 minutes.

TABLE 1 Standard Viscosity Test Conditions

Type Rubber[A]	Sample Preparation, See Section	Test Temperature, °C[B]	Running Time, min[C]
NBS 388	8.1 only	100 ± 0.5 or 125 ± 0.5	8.0
NR	8.1 and 8.2.1	100 ± 0.5	4.0
BR CR IR NBR SBR	8.1 and 8.2.2	100 ± 0.5	4.0
BIIR CIIR IIR	8.1 and 8.2.2[D]	100 ± 0.5 or 125 ± 0.5[E]	8.0
EPDM EPM	8.1 and 8.2.2	125 ± 0.5	4.0
Synthetic rubber black masterbatch	8.1 and 8.2.3	100 ± 0.5	4.0
Compounded stock reclaimed material	8.1 only	100 ± 0.5	4.0
Unmassed sample	8.1 and 8.3	Use conditions listed above for type rubber being tested.	
Miscellaneous	If similar to any group above, test accordingly. If not, establish a procedure.		

[A] See Practice D 1418.
[B] Test temperatures are 100 ± 0.5°C (212 ± 1°F) or 125 ± 0.5°C (257 ± 1°F).
[C] Time after the standard 1.0-min warm-up period at which the viscosity measurement is made.
[D] If no air bubbles are visible in the sample, 8.2.2 may be omitted.
[E] Use a temperature of 125 ± 0.5°C (257 ± 1°F) whenever specimen has a viscosity higher than 60-*ML* 1+8(100°C).

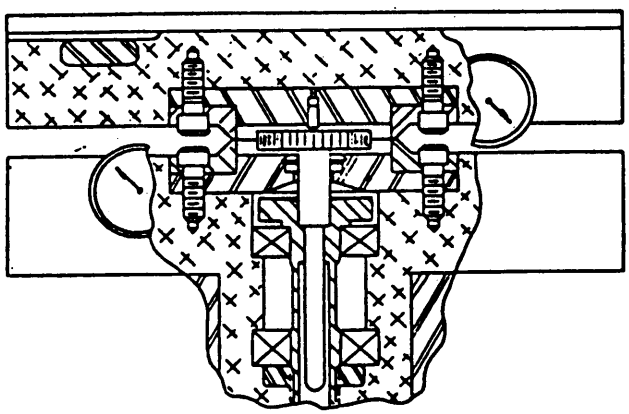

Figure 11. Mooney viscometer cross-section.

ELECTRICAL MEASUREMENTS

In order to measure electrical properties samples 0.5″ X 1″ X 1″ in dimension were prepared. The faces of the rubber specimens were coated with silver paint in order to serve as electrical contacts. A Hewlett Packard 0 - 10 volt power supply which was used to applu a potential across eacj sample. A Keithley logarithmic picoammeter was used to measure the resultinf current. A copper constantan thermocouple was taped directly to the sample, which was placed into a 2″ diameter metal chamber with steel disks above and below. The sample's electrical leads went through a hole in the side of the chamber to the power supply. The chamber was wrapped in heating tape regulated by a Powerstat variable autotransformer to control the sample temperature. this apparatus was then placed on a Revere 0 - 500 lb. load cell in a Greenerd 2 ton press. A Cole Parmer 2-pen chart recorder was used tto simultaneously record sample pressure from the load cell and sample current from the logarithmic picoammeter. This set-up is shown in figure (12).

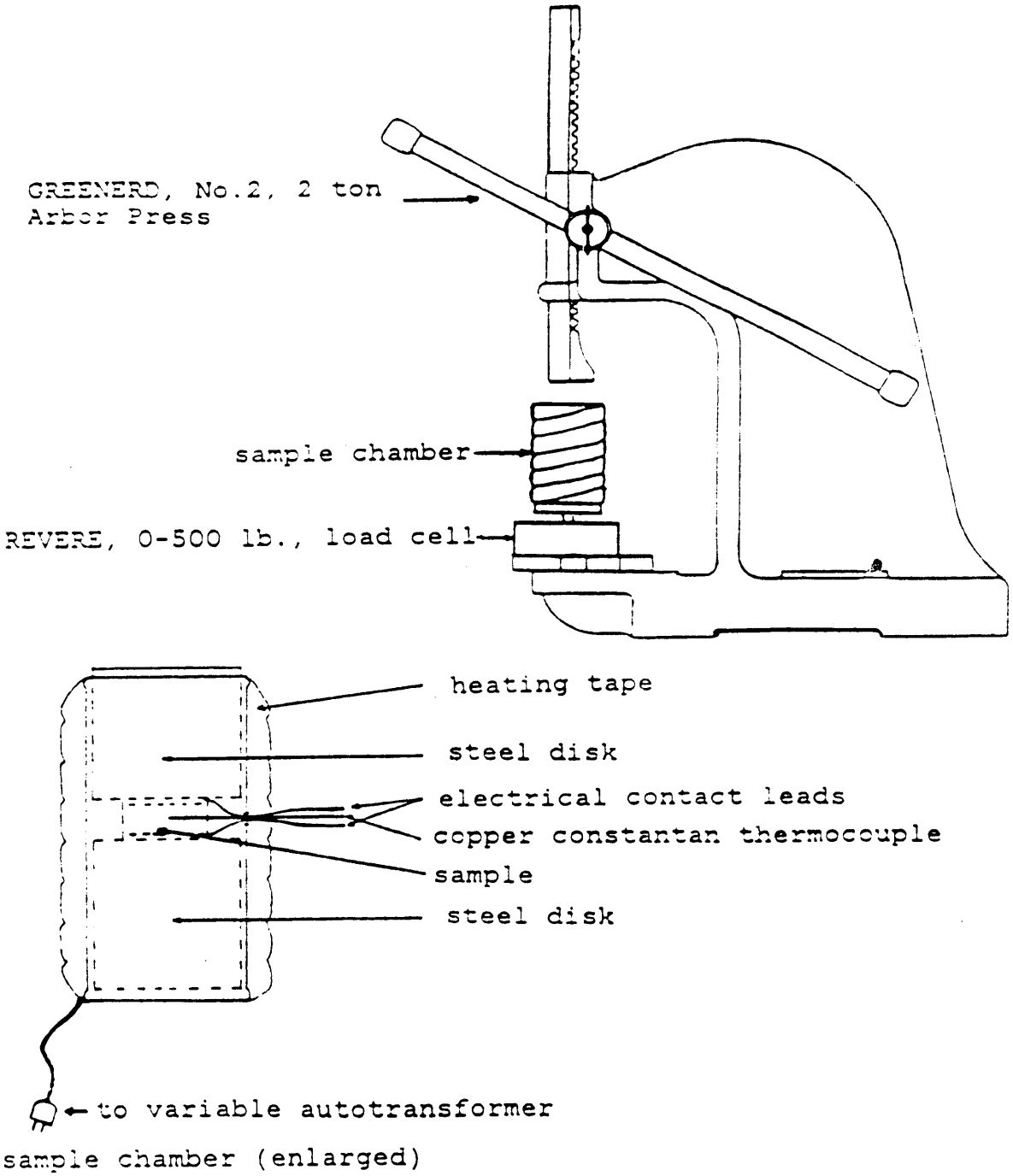

Figure 12. Apparatus used in electrical measurements.

3.1.3 DESCRIPTION OF SURFACE ANALYTICAL CAPABILITIES

3.1.1.7 DESCRIPTION OF S(T)EM

A Phillips 420 Scanning Transmission Electron Microscope was used to characterize the surface of the rubber as well as the morphology of carbon black in the various specimens. To perform the former, the scanning (SEM) mode was used while the latter was studied using the transmission (TEM) mode. In the scanning mode an electron beam of approximately 80A° diameter is used to illuminate the specimen. As the beam scans the surface, a variety of interactions take place with atoms on the surface and high energy back scattered electrons, low energy secondary electrons, X'rays and radiations in the ultraviolet, visible and infrared regions are emitted (38). Each of these carries some information about the nature of the specimen. All the interaction products can be monitored using suitable detectors. The signals formed in the detectors are suitably amplified and used to control the brightness of the CRT (intensity modulation). The scan coils of the microscope and the CRT are driven by the same scan generator, so that for each beam position on the specimen there is a corresponding position on the CRT; thus resulting in a one to one correspondence between any point on the specimen and the CRT. Schematics of SEM and TEM are shown in figures (13) and (14).

Since the interaction varies from point to point on the surface, there is a difference in the signal produced by the detectors as a result of which different values of brightness are obtained at different points on the CRT. In this manner the S(T)EM is capable of mapping on a screen areas scanned on a specimen.

In order to study carbon black morphology ultra-cryomicrotomed sections of rubber were examined on the S(T)EM using the transmission (TEM) mode. In this mode a static electron beam at 100 kv is focussed on the specimen which is approximately 400A°- 1000A°thick. If the section is thin enough then the electron may either pass through with its initial energy and direction or it may collide with other electrons and scatter them in the forward direction. An electron passing through can interact with the atomic nucleus. The relatively light weight of the electron causes it

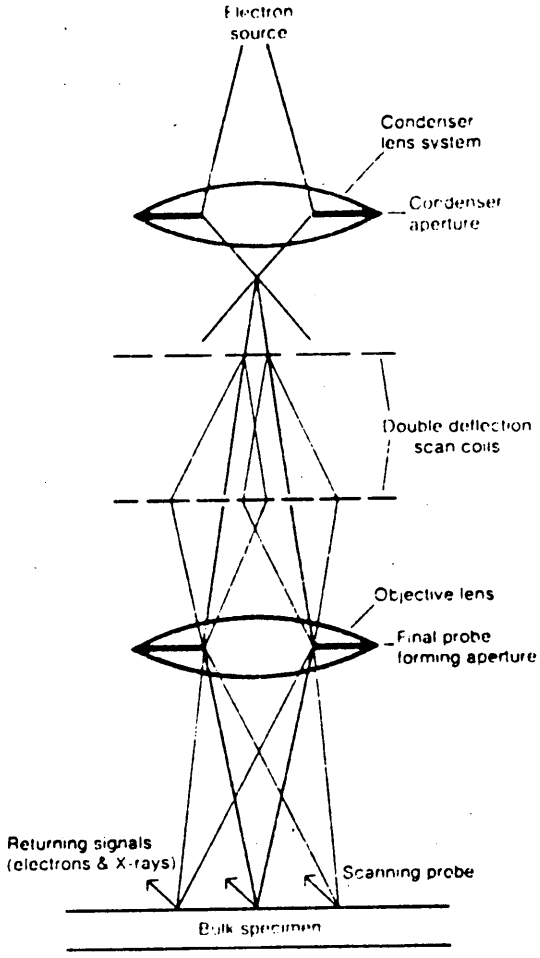

Figure 13. Electron Optical system of a SEM.

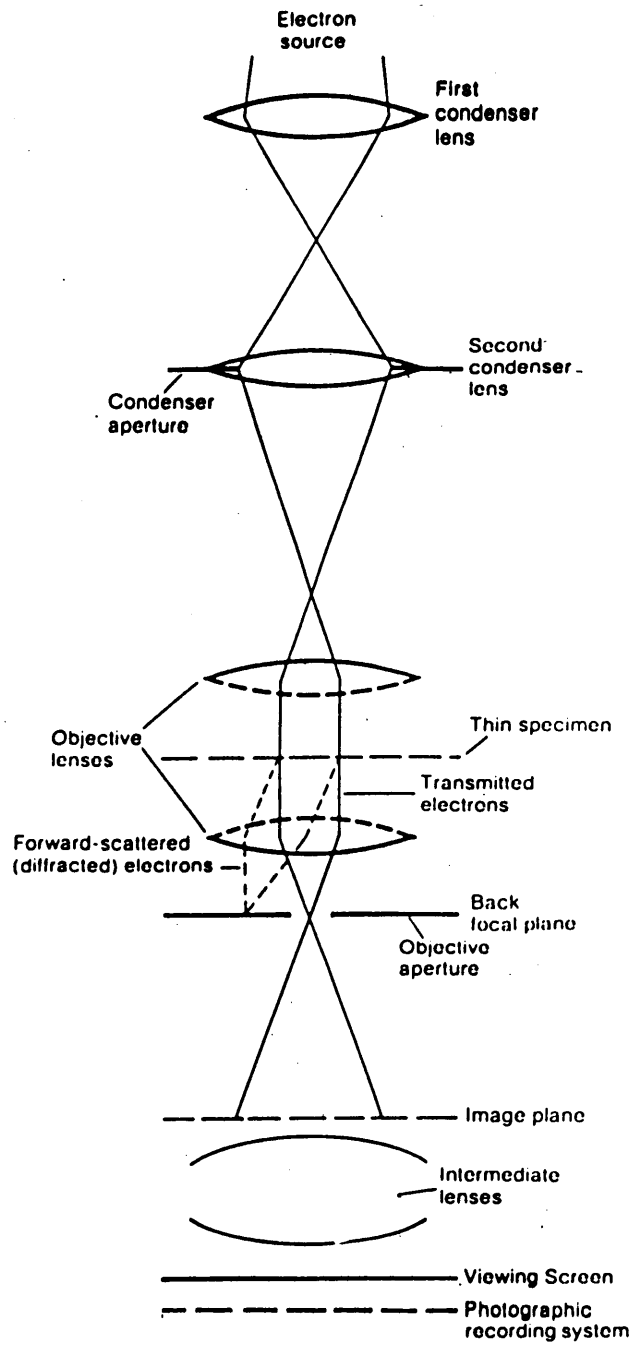

Figure 14. Electron Optical system of a TEM

to suffer a change in direction without a transfer of energy to the sample. This is referred to as an elastic collision. Both the transmitted and the forward scattered electrons are brought to a focus on the fluoroscent screen by the objective lens system. An image is produced in a electron microscope because of the variations in intensity produced on the fluoroscent screen. These variations may be produced as a result of one or more of the following effects - amplitude modulation, edge effects, refraction, diffraction, and miscellaneous deflecting fields.

3.1.1.8 ENERGY DISPERSIVE ANALYSIS OF X'RAYS:

A Tracor Northern TN 5500 Energy Dispersive X-ray Spectrometer was used to provide qualitative information about particulates and other inhomogenities seen in the electron microscopic investigations of the rubber compounds. When an incident electron in an electron microscope ejects an electron from the inner shell of an atom a vacancy is created. This vacancy is usually filled by an electron from a higher energy level dropping to the lower energy level. In dropping to this lower energy state the vacancy filling electron must give up some of its energy which appears as electromagnetic radiation. The energy of the emitted radiation is equal to the difference between the energy levels involved. This difference is quite large for inner shells and hence radiation is emitted in the form of X'rays (39). Figure (15a) shows the actual electron transitions in the atom and the subsequent emission of X'ray flourescence.

This X'ray emission is converted into a digital spectrum by a series of electronic components shown in figure (15b). Each X'ray photon creates a charge pulse in a semiconductor detector, which is converted into a voltage pulse of amplitude equal to the energy of the detected X'ray. Finally, this voltage pulse is converted into a digital signal, which causes one count to be added to the corresponding channel of a multichannel analyser. After a time, the accumulated counts from a sample produce an X'ray spectrum like those shown in figures (26, 27, 28). The information obtained from EDXS is at the most only semi-quantitive.

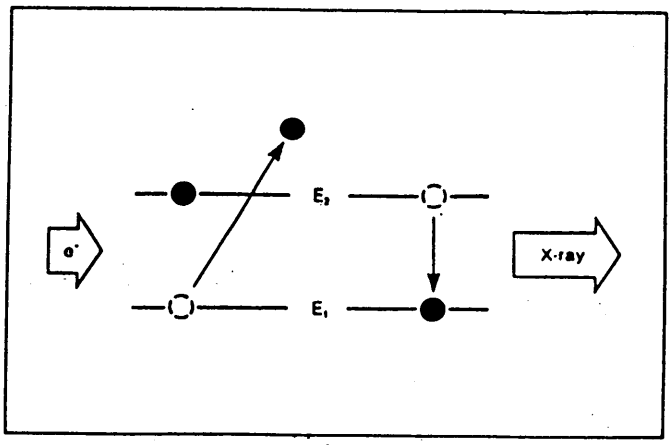

(a)

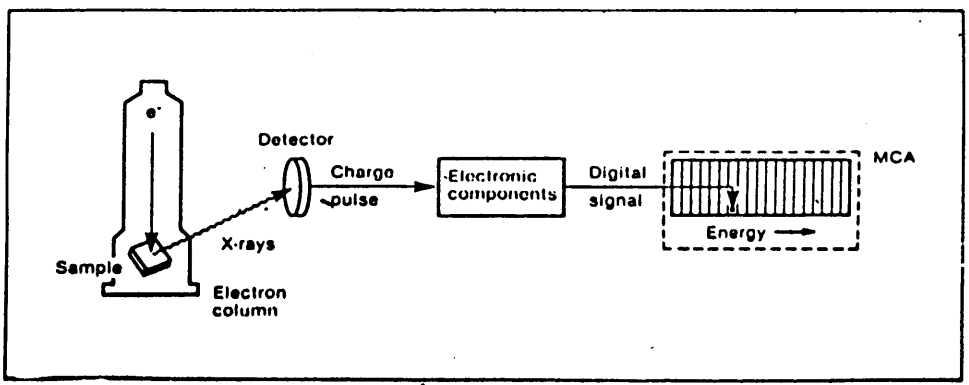

(b)

Figure 15. a) Shows electron interactions which result in X-ray fluorescence. b) Displays method of detection.

3.1.1.9 CRYO-ULTRAMICROTOME:

The ultramicrotome is used to microsection samples for viewing and analysis in the TEM mode. This instrument makes use of a glass or diamond triangular shaped knife which slices off thin sections of the specimen. The glass knife has a trough just behind its cutting edge which contains a liquid to collect the sections. The specimen is mounted on an arm which moves vertically from top to bottom past the glass knife. The thickness of the specimen can be adjusted to a certain degree by means of a knob on the monitor. The cryoultramicrotome has a freezing accessory which can be used to freeze sections and then cut them. The temperature of the object and knife can be controlled separately from + 40°C to -160°C with an accuracy of + 0.2 °C. The figure (16) clearly shows the working of the microtome.

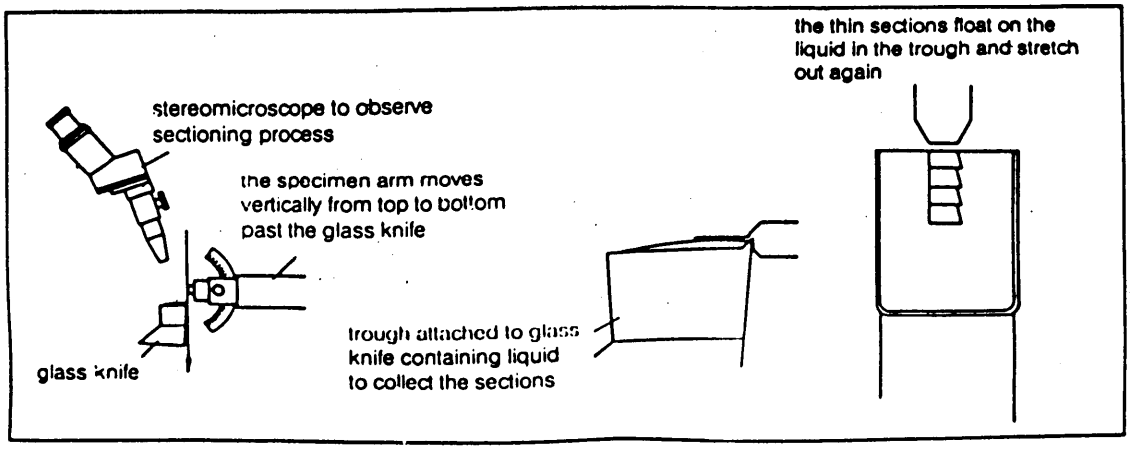

26 Preparation of ultra-thin sections. Diagram of a microtome with triangular glass knife

Figure 16. The working of the cryo-ultramicrotome.

3.1.1.10 X-RAY PHOTOELECTRON SPECTROSCOPY:

A Kratos XSAM 800 was used to investigate the chemical composition of the surface and bulk of rubber compounds as well to perform ion sputtering on the samples. The XPS consists of an X-ray gun which emits photons. These incident photons interact with the surface atoms producing photoelectrons and Auger electrons. These interactions are shown below in figure (17). Electron emissions are detected by an electron spectrometer according to their kinetic energies. The analyser is operated as an energy "window", accepting only those electrons within the range of this fixed window, referred to as the pass energy. Scanning for different energies is accomplished by applying a variable electrostatic field, before the analyser is reached. This retardation voltage may be varied from zero up to the photon energy. Electron are detected as discrete events, and the number of electrons for a given detection time and energy is stored digitally (40).

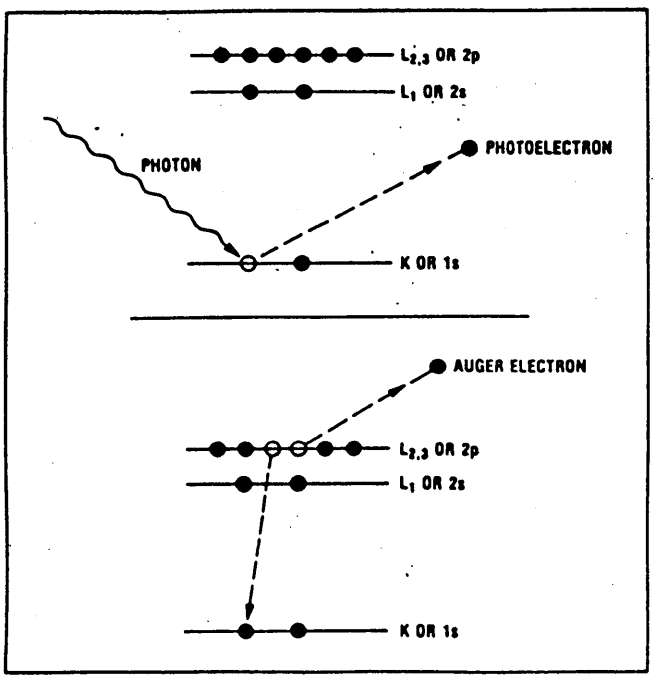

Figure 17. Interactions between photons and electrons which give photoelectrons and Auger electrons.

Chapter 4

4.0 RESULTS AND DISCUSSION

4.1.1 MOONEY VISCOMETER:

The results of the Mooney viscosity tests were as follows.

	A-2	A-1	B-1	C-1	D-1	E-1	F-1	G-1
INITIAL	112.0	136.0	139.0	200+	200+	200+	200+	200+
1.5 Minutes	71.5	85.5	91.5	135.5	148.5	158.5	154.5	159.5
4.0 Minutes	55.0	75.0	79.0	118.0	124.0	148.0	144.0	147.0

Table 4. Mooney Viscosity during curing at 1.5 minutes and 4.0 minutes.

The above results show that the order of addition of ingredients has a pronounced effect on the viscosity. While a high viscosity is favorable for obtaining a good dispersion because it gives rise to high shear forces during the mixing, too high a viscosity can be detrimental to the dispersion because the mixture becomes unprocessible. The initial viscosities for C-1, D-1, E-1, F-1 and G-1 were very high and their upper limits were undeterminable using the large disc. As mixing time is increased the viscosity begins to decrease which is expected. A Mooney scorch test was also

performed to determine how 'safe' the compound was. The term 'safe' is used here to mean how long a compound can be subjected to mixing before it begins to cure because of the high temperatures developed in the mixer. In order to measure this the disc is rotated until the lowest possible viscosity is measured. Rotation is continued until the viscosity increases five points. The time taken for this to occur is noted down. This is called the Mooney scorch time, and was rather 'short' for the experimental rubber compounds. However the abrasion and blowout resistance properties are improved i. e. these are obtained at the cost of some of processing safety. The results of the Mooney scorch viscosity tests performed at 250°F using the large disc is as follows:

	A-2	A-1	B-1	C-1	D-1	E-1	F-1	G-1
Minutes (+ 5)	13.5	14.0	16.6	10.0	9.2	12.5	12.4	12.6
Min. Viscosity	51.0	55.5	57.5	91.0	107.0	110.0	117.0	118.0

Table 5. Mooney Scorch viscosity at 250°F.

4.1.2 ELECTRICAL PROPERTIES:

Electrical properties viz. resistance and conductance of all the samples were determined. These seemed to correlate to some extent with observations made in the photomicrography. The resistance for well dispersed samples is usually higher than for the not so well dispersed samples as can be seen in table (6) and figure (18). Samples were gold plated and the resistance was measured. Following table shows the resistance obtained on the gold plated samples.

SAMPLE	Ro(Ohm)	R1(Ohm)	R3(Ohm)	R4(Ohm)
A2	159	344	754	400
A1	137	197	372	235
B1	125	167	272	192
C1	141	197	343	230
D1	157	292	611	365
E1	115	123	140	129
F1	114	120	136	126
G1	110	116	123	118

Table 6. Relaxation resistance of gold plated samples.
Ro - Initial resistance
R1 - Resistance at the beginning of 150lbs applied.
R3 - Resistance at the beginning of 150lbs released.
R4 - Resistance at time (t = 300 seconds) after 150lbs is released.

This is because when a sample is well dispersed there exists no continuous conductive network of carbon black throughout the compound while for improperly dispersed samples there are many such strands which provide conductive paths thereby decreasing the resistance.

The histogram of measured resistance for the various samples shows that samples A-2, A-1 and B-1 shows a linear trend with mixing time whereas C-1 and D-1 show a deviation from this trend. Sample D-1 shows unexpected behaviour; resistance measurements indicate that the dispersion for it is as good as A-2. Photomicrographs of carbon black morphology in figure (36 and 37) show clearly that the dispersion of D-1 is better than C-1. Samples E-1, F-1 and G-1 show a relatively low resistance which is expected for bad dispersions. The increase in resistance after the application of the 150lbs load is due to the disruption of the existing conductive network.

4.1.3 TENSILE TESTS

Dumbbell specimens were used for these tests. The dies used for preparing are as per ASTM D 412; the 'grain' has a bearing on the stress strain results and hence the specimen should be cut with their lengthwise direction parallel with the mill direction.

Tensile properties are a function of dispersion, which itself is a function of the quality of mixing, modulus was calculated at 100%, 200% 300% and at break. Tests were run at room temperature and 250°F.

A plot of modulus vs time of mixing for the various rubbers shows linear behaviour, with modulus increasing with the decrease in mixing time. This indicates a high stiffness for the rubber at low mixing times. This can be verified from the higher hardness values obtained during the durometer test as shown below.

	A-2	A-1	B-1	C-1	D-1	E-1	F-1	G-1
HARDNESS	75	76	76	77	77	78	78	79

Table 8. Shore A hardness from durometer tests.

An examination of the plots of modulus vs mixing time shows that there is a parallel shift in the modulus when measurements are made at 250°F. This shift is a negative one i. e. lower modulus values are obtained at higher temperatures, which is expected. There is a parallel shift in modulus at 100% elongation of 177.5 psi and at 200% elongation of 233.7 psi. The 300% moduli do not show a parallel shift; compounds E-1, F-1 and G-1 fail even before 300% elongation is acheived. This is because these compounds have bad dispersions, with a large number of carbon black agglomerates acting as stress risers as a result of which they fail even before 300% elongation is reached, when tested at 250°F. Plots are shown in figures (19), (20) and (21).

Dispersion of black within the rubber is found to occur within two stages a) the first one in which black is encapsulated by the rubber and b) the second stage in which the voids in the black are penetrated by the rubber and the black is dispersed. In the case of samples C-1, E-1, F-1 and G-1 there appears to be large agglomerates of undispersed black whose interstices are not well penetrated by the rubber (refer figures 36-40). This results in large agglomerates of carbon black

	A-2	A-1	B-1	C-1	D-1	E-1	F-1	G-1
MODULUS @ 100 PSI	420	440	460	610	840	930	1000	1000
250°F	330	330	320	470	569	680	810	780
MODULUS @ 200 PSI	1070	1030	1100	1410	1710	1810	2060	2140
250°F	790	840	800	1160	1390	1680	1940	1920
MODULUS @ 300 PSI	1970	2050	2130	2650	2910	3350	2930	3300
250°F	1620	1750	1760	2050	2220	--	--	--
TENSILE STRENGTH, PSI	3320	3520	3180	3180	3410	3350	2930	3300
250°F	2480	2550	2350	2380	2210	2210	1940	1760
ELONGATION%	475	% 425	425	350	320	300	300	300
250°F	420	420	420	320	300	240	200	200

Table 7. Unaged stress strain properties.

being loosely held together by the surrounding rubber as can be seen from the photomicrographs (37, 38, 39) shown below. These cause a very weak carbon black network in the rubber, which disrupts easily on the application of a large stress; further the lack of proper dispersion gives rise to inhomogenities which can act as stress concentration points leading to an early failure .

Aged stress strain properties were determined by keeping samples for 70 hours at 212°F according to ASTM D 573.

The samples A-2, A-1, B-1, C-1, D-1 and E-1 show an increase in modulus with ageing, which probably indicates that hardening occurs when the sample is heated for extended time periods. This can be seen from the durometer hardness measurements made after the ageing has taken place.

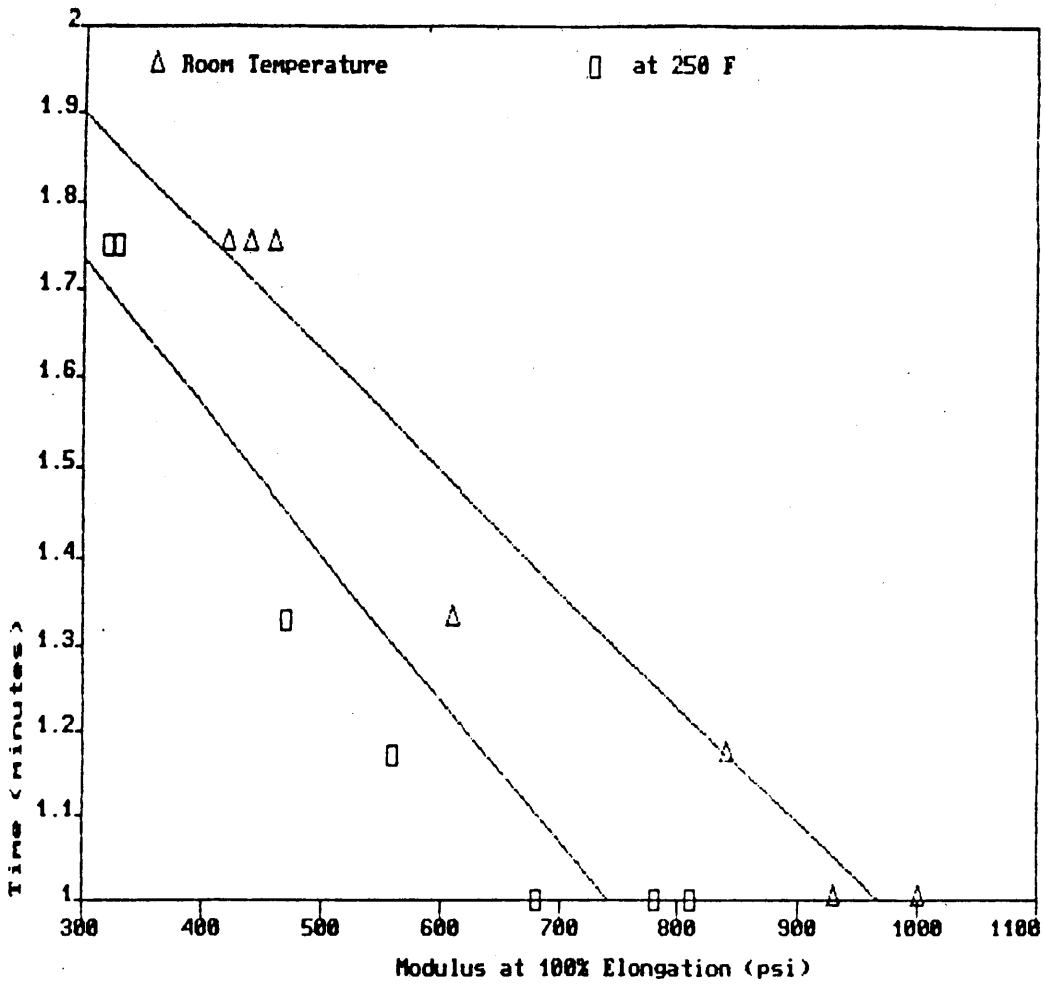

Figure 18. Plot shows the shift in Modulus at 100% elongation

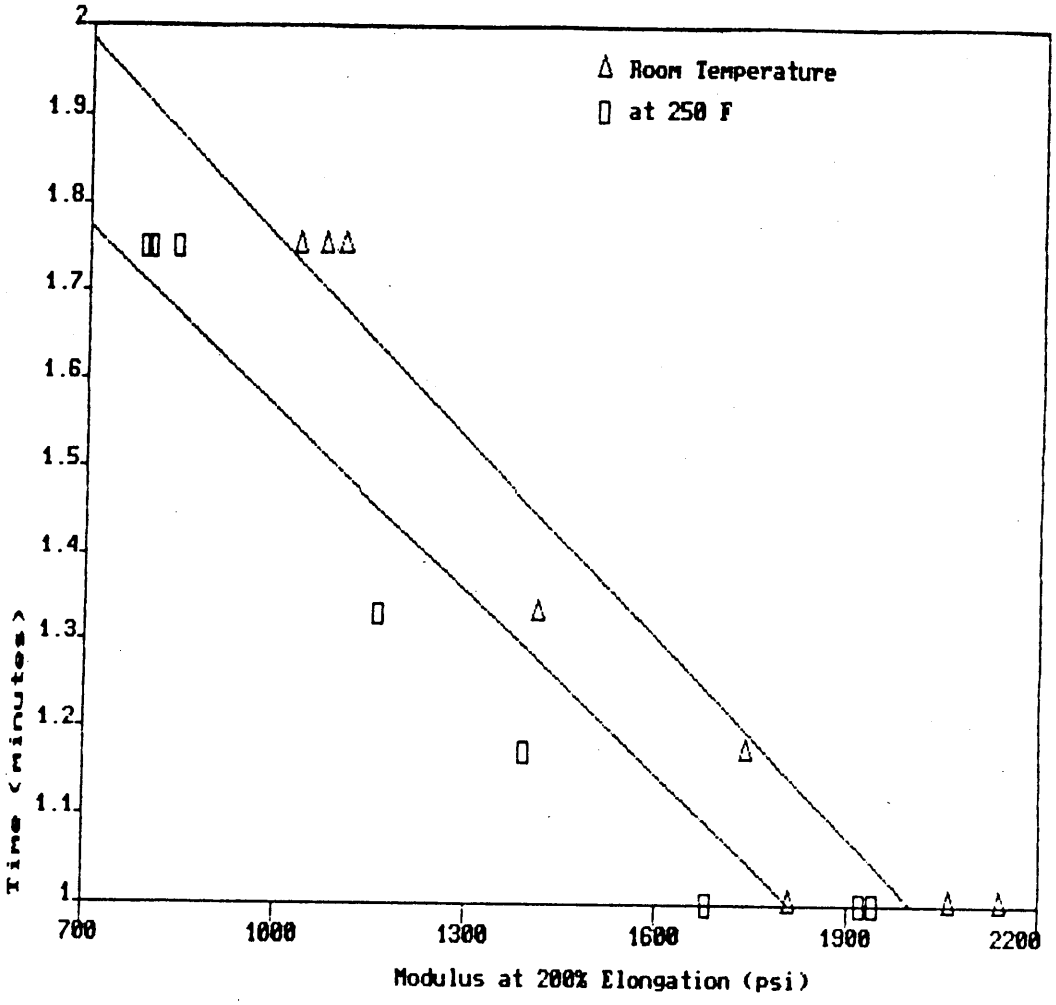

Figure 19. Plot shows shift in Modulus at 200% elongation.

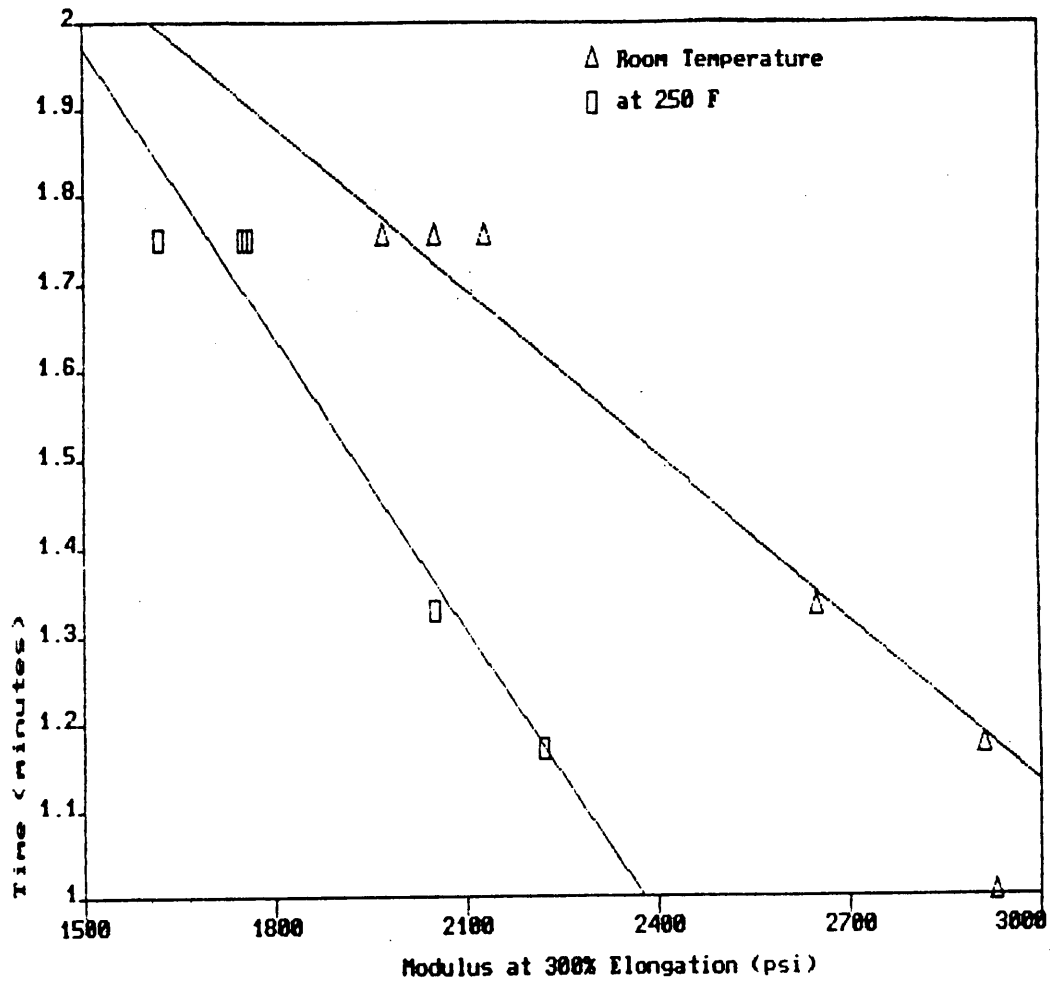

Figure 20. Plot shows shift in modulus at 300% elongation.

	A-2	A-1	B-1	C-1	D-1	E-1	F-1	G-1
MODULUS @ 100 PSI	710	730	710	820	1000	1040	1000	1160
MODULUS @ 200 PSI	1620	1550	1590	1980	2030	2460	2100	2380
MODULUS @ 300 PSI	2670	2570	2510	3160	3260	--	--	--
TENSILE STRENGTH, PSI	3300	3130	3330	3260	3260	3230	2570	2860
ELONGATION%	380	380	380	320	300	270	250	240

Table 9. Aged stress strain properties.

	A-2	A-1	B-1	C-1	D-1	E-1	F-1	G-1
HARDNESS	80	81	81	82	83	84	84	85

Table 10. Shore A hardness from durometer tests after ageing.

This increase in the hardness is attributable to the oxidative degredation which takes at an accelarated rate at higher temperatures.

DIE B TEAR RESISTANCE

The results of these tests conducted as per ASTM D 624 are as follows:

	A-2	A-1	B-1	C-1	D-1	E-1	F-1	G-1
RT	375	337	374	340	334	289	297	270
250&DEG.F	212	178	184	159	150	153	151	148

Table 11. Tear resistance in lbs/inch.

Some trends noted earlier are seen again i. e. the linearity of the results with mixing time. Sample B-1 shows better resistance to tear than A-1; this can be attributed to inhomogenities which vary from sample to sample but yet play an important role in the overall physical properties and the ultimate performance of the compound. At room temperature there is a wide difference in the tear resistance behaviour exhibited by the well dispersed samples A-2, A-1 and the badly dispersed samples E-1, F-1 and G-1. When the test is conducted at 250°F the tear resistance decreases. However the decrease in resistance is almost equal for all the samples and is around 45%. This indicates that the quality of dispersion does not play a very important role in the change in tear resistance which takes place due to increased higher temperatures. This behaviour suggests that the affect of high temperature on the base matrix is very significant and performance of a rubber compound at these elevated temperatures hinges largely on the state of the vulcanisate at that temperature rather than the quality of the dispersion.

An important factor to be looked into here is the tear resistance vs the abrasion characteristics. It can be seen that while badly dispersed samples show better abrasion resistance than the well dispersed samples they display a much lower hot tear strength. The poor quality dispersion samples show a very high viscosity, high modulus, poor tear strength but a good resistance to abrasion. In this case samples E-1, F-1 and G-1 had a very high viscosity initially as determined from the Mooney viscosity experiments. This viscosity was too high to be utilised to improve the quality of dispersion (since a high viscosity provides for higher shear forces in the mixing system) and the effects of this can be seen in the electrical and physical properties.

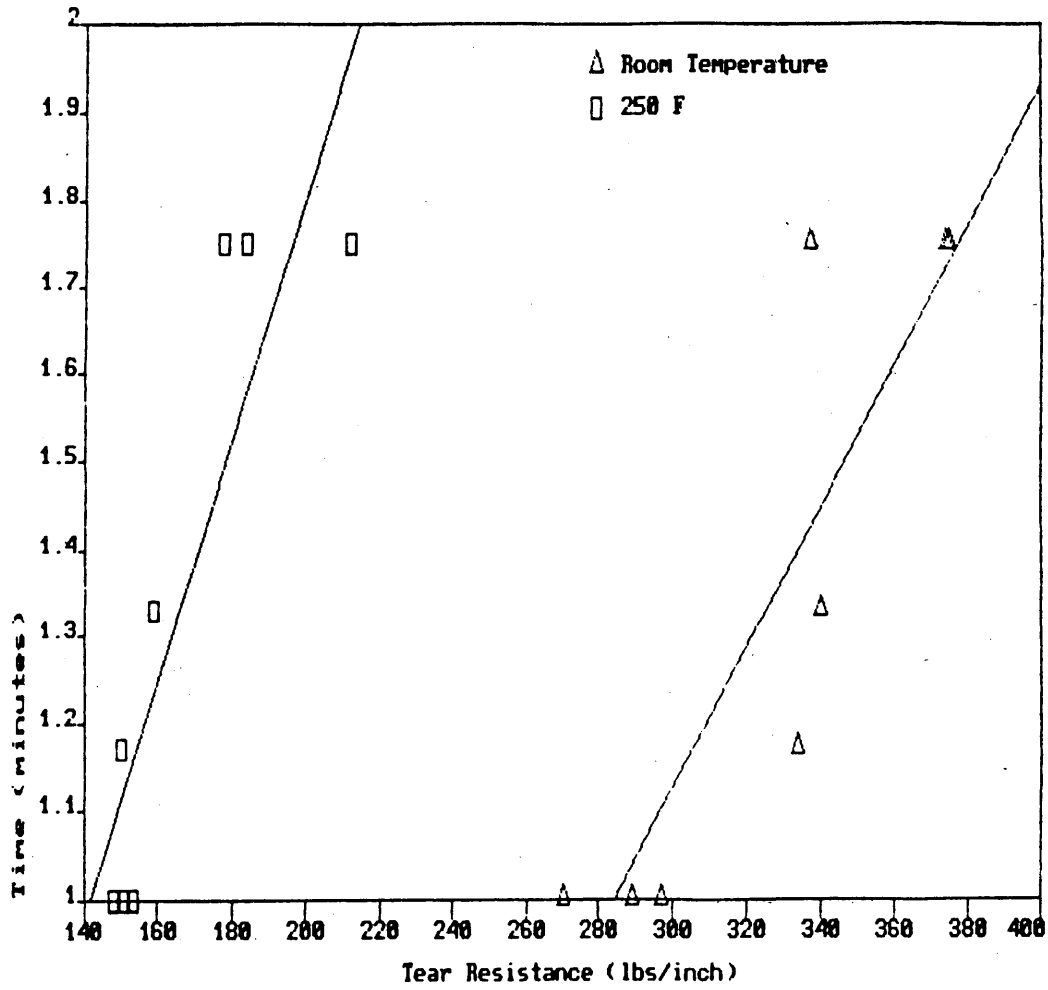

Figure 21. Tear resistance varies in a linear fashion with mixing.

4.1.4 ABRASION RESISTANCE:

The results of the abrasion tests were as follows:

	A-2	A-1	B-1	C-1	D-1	E-1	F-1	G-1
PICO RATING	155	151	159	162	169	177	176	175

Table 12. Pico abrasion resistance for various samples.

The Pico ratings show that the samples A-2, A-1, B-1 which are well dispersed undergo more abrasion and weight loss than samples E-1, F-1 and G-1. This is due to the fact that the latter samples have bad dispersions and are harder, as can be seen from the durometer tests. As a result of this increased hardness, wearing of the surface does not take place easily. Again it may be seen that the abrasion properties vary almost linearly with mixing time.

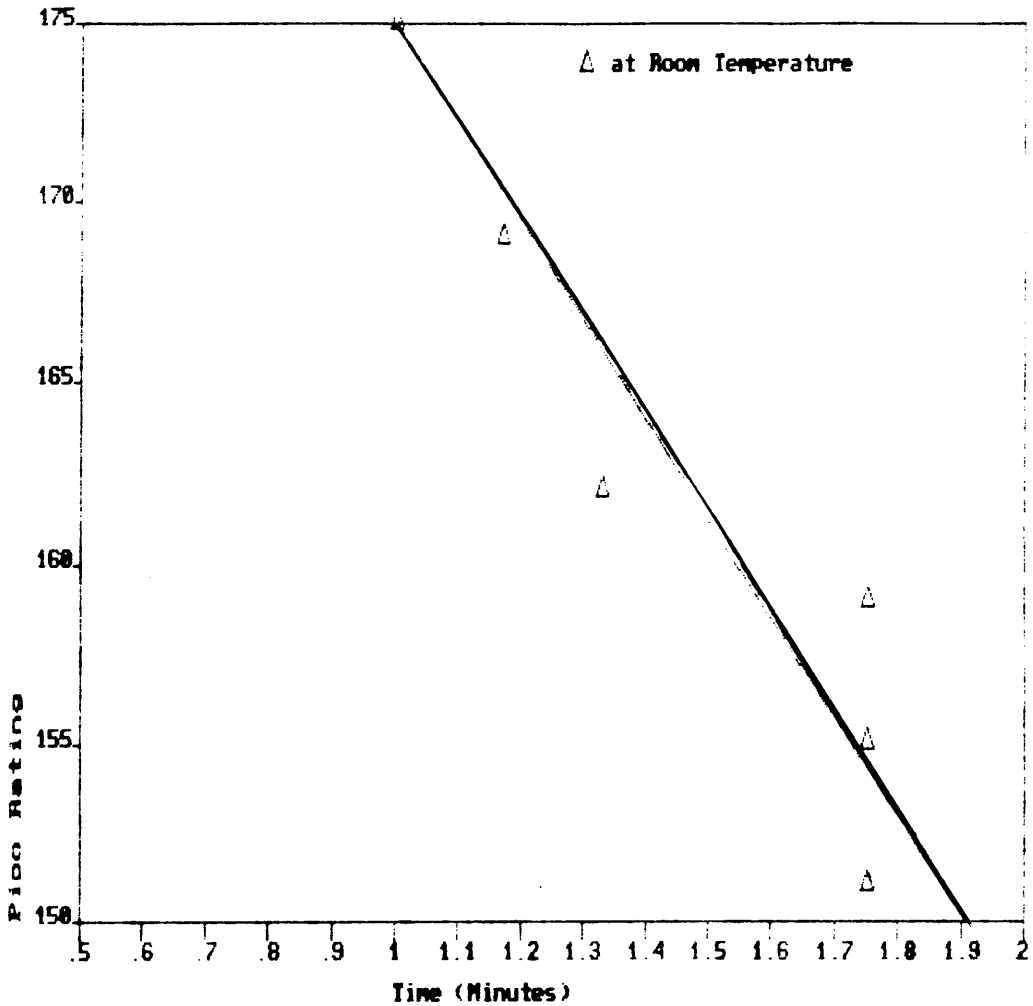

Figure 22. Abrasion results plotted against the time of mixing.

4.1.5 DEMATTIA FLEX TEST

The results obtained on this test was as shown below.

	A-2	A-1	B-1	C-1	D-1	E-1	F-1	G-1
	11.7	6.0	2.9	2.4	0.6	0.2	0.2	0.2
	3.1	3.0	4.1	2.3	0.7	0.2	0.2	0.2
	3.0	2.0	1.6	0.8	0.6	0.2	0.2	0.2
AVERAGE	5.9	3.7	2.9	1.9	0.6	0.2	0.2	0.2

Table 13. DeMattia flex cut growth resistance in kilocycles/0.1 inch cut growth.

The average flex cut growth resistance varies with the dispersion. Sample A-2 shows the highest resistance followed by the other samples in the order of the quality of the dispersion. The three readings taken show a large scatter. This can be attributed to the heterogeneous nature of the compound itself. Readings are likely to be influenced by the presence of particulates such as sodium chloride, calcium, magnesium and sulfur which have been identified using EDX spectrometry on the other failure surfaces.

4.1.6 GOODRICH FLEXOMETER

Cylindrical rubber samples 25mm ± 0.15mm. in height and 17.8mm + 0.1mm in diameter (as per ASTM D 623) were cured for 45 minutes at 325 deg F, typical of the cure at the center of the production tank track pad. The samples were then subjected to flexing for different time periods as follows: a) First five samples of each type were flexed at 440psi and 30cycles/second until blowout. The experiment was repeated with different samples of similar mixing conditions but flexed at 200psi and 30cycles/seconds, in order to study the effect of load on heat build up. b) Samples were flexed at 440psi and 30cycles/second for time periods ranging from 0.5 min. to blowout to study the formation and propagation of cracks and voids. During flexing the rise in temperature was noted down as was the time taken to blowout. Subsequently plots were made of time vs temperature for each sample. A plot for sample B-1 is shown in figure (24).
Samples showing different trends were analyzed for dispersion quality using the TEM.

These samples were flexed at 440 psi. The time vs temperature graphs showed that for each set of samples i. e. A-1, B-1 and C-1 there were some specimens that showed different trends.

Sample No.	Flexed Time	Condition
1	2.5 min.	4
5	3.6 min.	4
6	3.0 min.	1
7	2.5 min.	4
8	2.5 min.	1

Table 14. Blowout data for A-1.

In the above table, integers were used to indicate the condition of the samples after flexing. These are as follows:

Sample number (1) was chosen since it took a short time to blowout. This sample was split open and examined on a scanning electron microscope and a transmission electron microscope. Examination in the SEM revealed that the blowout surfaces were flaky and had macro-cracks as can be seen in the photograph (36b). A large number of brittle like failure regions were seen and also regions where failure was initiated. These are shown in photographs (38). The reason for the brittle like appearance could be due to oxidative scission and recrosslinking which has been reported

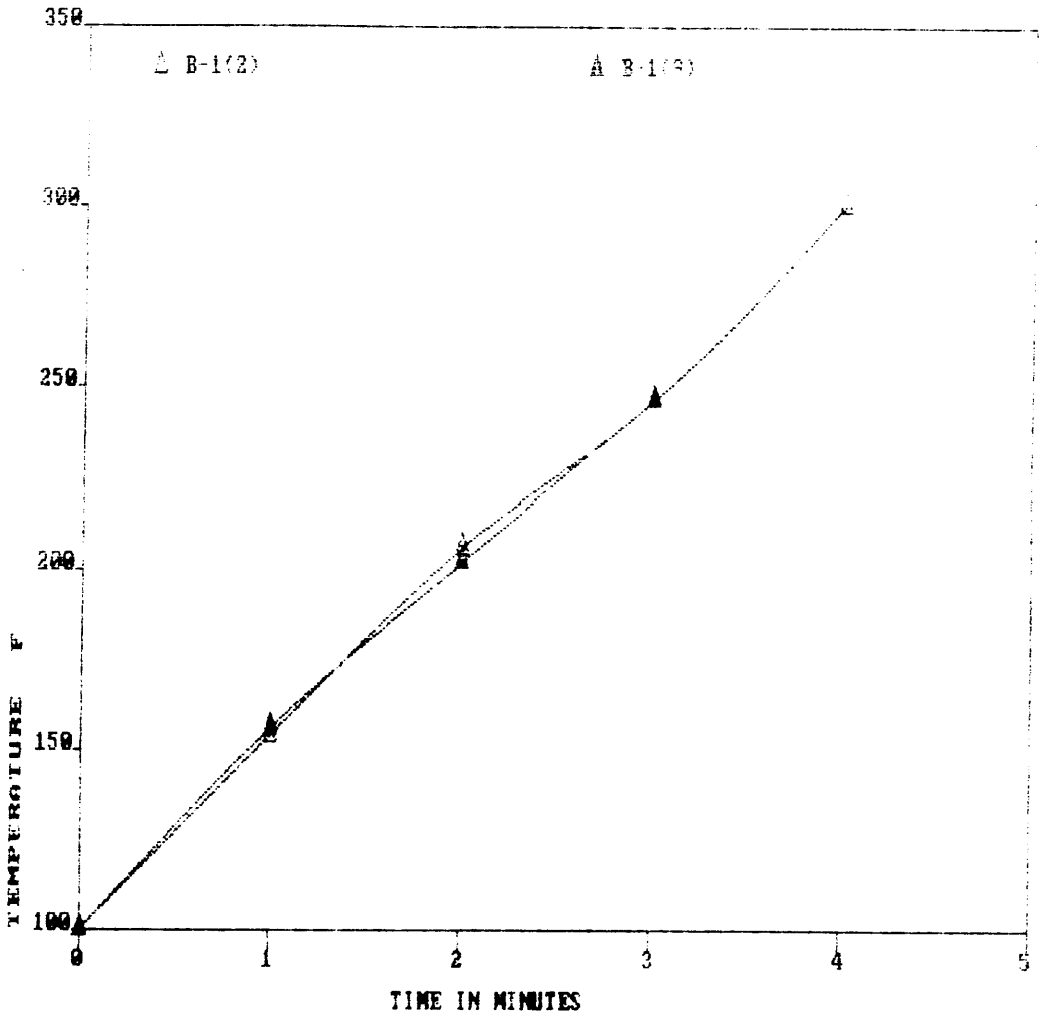

Figure 23. Plot shows that samples (2) and (9) have different heat transfer characteristics.

Condition	Description
1	Very slight blister
2	Slight blowout
3	Moderate blowout
4	Large scale blowout

Table 15. Symbols used to characterize various conditions.

by several authors (18,19). This recrosslinking causes an increase in the crosslink density (42) which results in increased embrittlement. Photographs in figure 37 (a), (b), (c) and (d) of blowout samples show a surface with a network of rectangular cracks; The surface appears almost glassy. This glassy appearance is also due to the brittleness caused by crosslinking.

The appearance of glassy behaviour is due to the combination of an increase in the crosslink density which causes an increase in Tg as well as the fact that the Tg is shifted to a higher temperature during the flexing. It is most likely that the polymer is now in the glassy regime and hence most of the failure surfaces seen in the flexometer samples have a brittle like appearance.

Specimens (2) and (9) were cut and examined from sample B. This sample showed a large number of voids, several of which seemed to propagate into cracks. The data for sample B-1 is shown below.

Sample No.	Flexed Time	Condition
9	3.0 min.	2
10	2.3 min.	1
11	2.7 min.	2
12	3.0 min.	3
2	4.0 min.	4

Table 16. Blowout data for sample B-1.

Data for samples C-1 and D-1 are shown below.

Sample No.	Flexed Time	Condition
4	3.5 min.	4
13	3.3 min.	3
14	3.6 min.	3
15	3.4 min.	3
16	3.0 min.	3

Table 17. Blowout data for sample C-1.

Sample No.	Flexed Time	Condition
35	2.9 min.	1
13	3.0 min.	1
14	2.9 min.	1
15	3.0 min.	1
16	2.9 min.	1

Table 18. Blowout data for sample D-1.

Sample D-1 was very rigid and hence kept jumping out of the flexometer before completion of the test, hence complete flexometer data could not be obtained.

The observation of a large number of voids and the development of these voids into cracks in the bulk of the material prompts a rationalisation of such behaviour. On flexing a specimen a large amount of heat is generated in the centre of the specimen. This heat is developed essentially due to a large amount of internal friction. The heat is dissipated at the surface. Depending upon the quality of the dispersion higher friction in certain regions gives rise to hot spots where radicals are released at high temperatures. Repeated scission in a particular region results in low molecular weight products being formed at these spots. These low molecular weight products decompose at higher temperatures 500-600°F to form gases. There is a considerable increase in the volume during its conversion from solid into gas. Thus a void is produced at the spot where the solid transitions into a gas. A large number of voids produced in the vicinity of one another would give rise to a considerable expansion in the volume. These microvoids themselves act as stress risers and the combination of these with the non-uniform strains to which the sample is subjected during the flexing result in an extremely high stress on the surface. The combination of these high surface stresses with the effect produced by the expanding gases and the accompanying high temperatures

results in a void propagating into a crack and eventually leading to a large scale blowout. The insides of blowout samples are always hollow containing a large number of cracks and a considerable amount of gas exits from the sample at blowout.

FLOW LINES: In order to study the heat build up in flexed samples studies were conducted on samples cycled for varying time periods from 0.5 minute to blowout. After flexing all the samples were cut open and examined under an optical microscope. It was seen that the well dispersed samples such as A-2, A-1, B-1 etc. had very few voids after 3 minutes of flexing while samples E-1, F-1 and G-1 had large scale cracks and a large number of voids. Sample E-1 was completely was completely blown out after 3.0 minutes of flexing. A surprising new observation was made here. The cut sections of the samples showed flow lines which are relatable to the processing. It was noted that the voids initiated and propagated into cracks along these flowlines. The large scale blowout observed in sample E-1 was observed to occur at the vortex of these flowlines. While it was seen that flowlines existed in all samples, these were more pronounced in samples which had bad dispersions. Hence a secondary effect of bad dispersions is that it tends to produce flow lines and seams where cohesive delaminations occur. Figures (25) shows the initiation and propagation of these voids and cracks along these flowlines. Figure (26) shows a large scale blowout which occured at the vortex of the flowlines.

Figure 24. Initiation and propagation of voids and cracks along flowlines.

Figure 25. Blowout which occured at the vortex.

4.1.8 ELECTRON MICROSCOPY

Scanning electron microscopy and transmission electron microscopy was performed to study the mechanisms of failure and the nature of failure surface. Noted in the SEM studies of blowout surfaces as well hot tear surfaces was the presence of calcium, magnesium, sulfur and sodium chloride in varying quantities (refer figures 27).

Photomicrograph 27(a) shows a large lump of sulfur from sample F-1, while in figure (b) a fairly large sodium chloride crystal is embedded in the rubber sample E-1. Photomicrographs (c) and (d) show calcium particulates present on the fracture surfaces of samples G-1 and F-1 respectively. Energy dispersive spectra from these particulates are shown figures (28) and (29).

In order to determine whether contaminants were concentrated at the failure surfaces or distributed throughout the bulk razor cut surfaces were looked at. It was found that there was a fairly coincentration of foreign particulates on these razor cut surfaces. Figures (32a) shows a square sodium chloride particulate ofside equal to 0.24 microns embedded in sample F-1, while figure (30b) shows an elliptical sodium chloride particulate whose major axis is approximately 22.5 microns embedded in the rubber sample G-1. A large sulfur particulate of size 4.8 micron is seen embedded in F-1.

In some cases a large concentration of contaminants were found on both fracture and razor cut surfaces as can be seen in figures (33) and (34). In figure (33) a large amount of contaminant was seen on the fracture surface of sample A-2. EDX identification of the particulates showed that they were composed mainly of calcium, magnesium, sulfur and silicon. In the photomicrograph (33c) the particulates are seen to be located in cracks. It is more likely that the particulate acted as a stress riser which gave rise to the crack during the hot tear. All the cracks are surrounded by halos. These regions were seen to very rich in sulfur. It is most probable that sulfur concentrates in the regions around the particulates, forming a region of high crosslink density and hence increased embrittleness, as can be seen from the flexometer photomicrographs (37). Photomicrographs shown in figures (34a) and (34b) show a large concentration of contaminants on the fracture surface. The razor cut surface examined in figure shows an equally large number of holes in which contaminant particulates resided. These particulates seem to have melted during some heating process e. g.

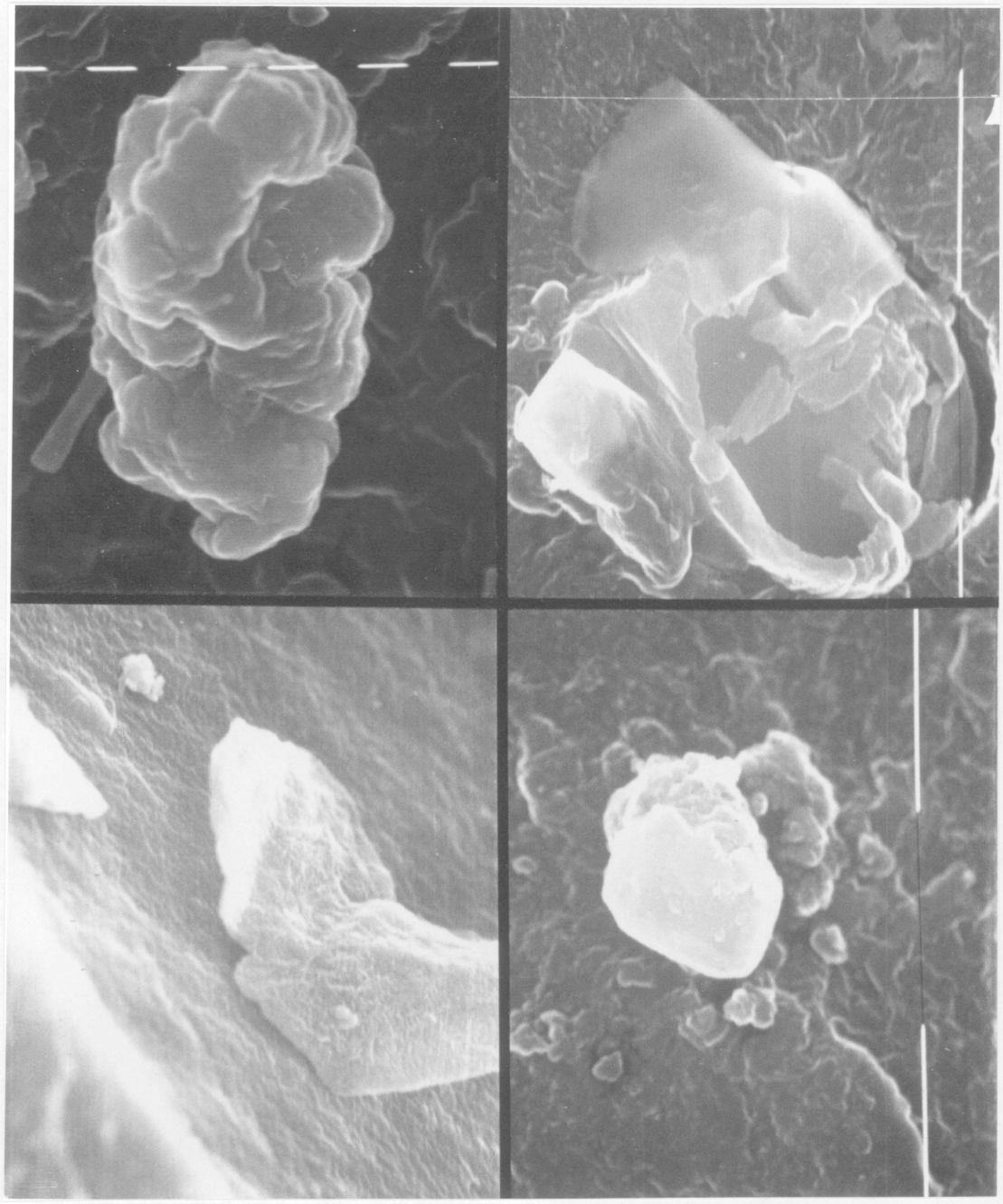

Figure 26. Contaminants found on the hot tear surface. a) Sulfur particle. Mag. 12500X b) Sodium Chloride at 6400X. 3) Calcium at 2400X. 4) Calcium at 6400X.

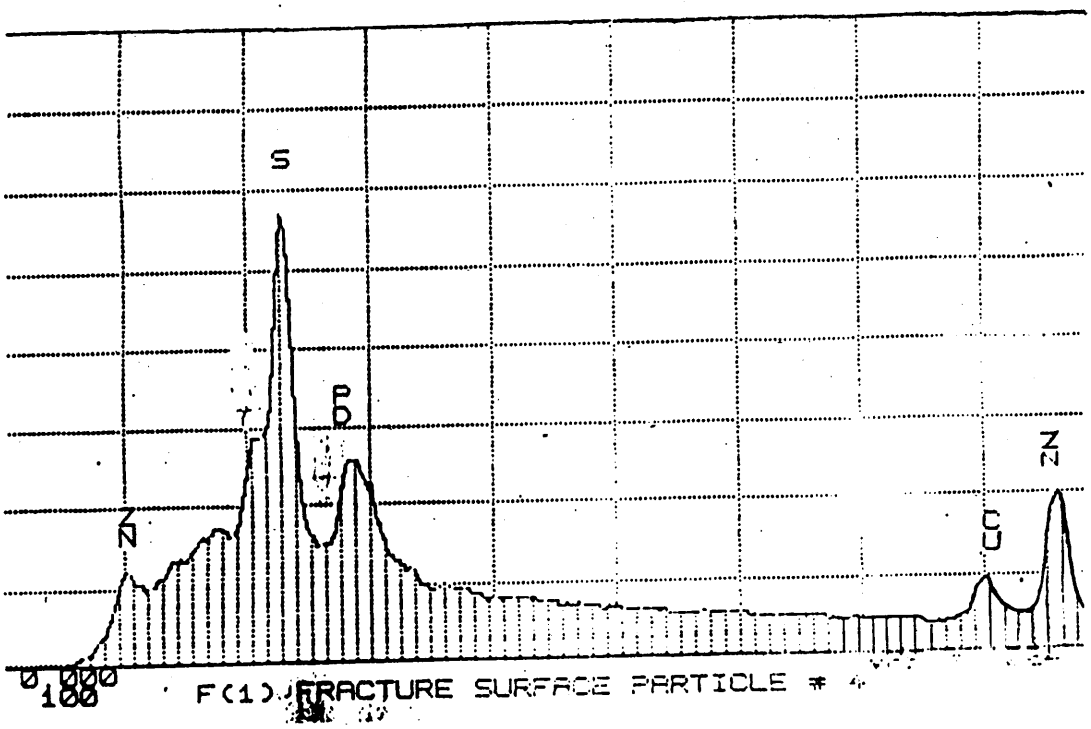

Figure 27. EDX spectra of particulates shown in figure (27a).

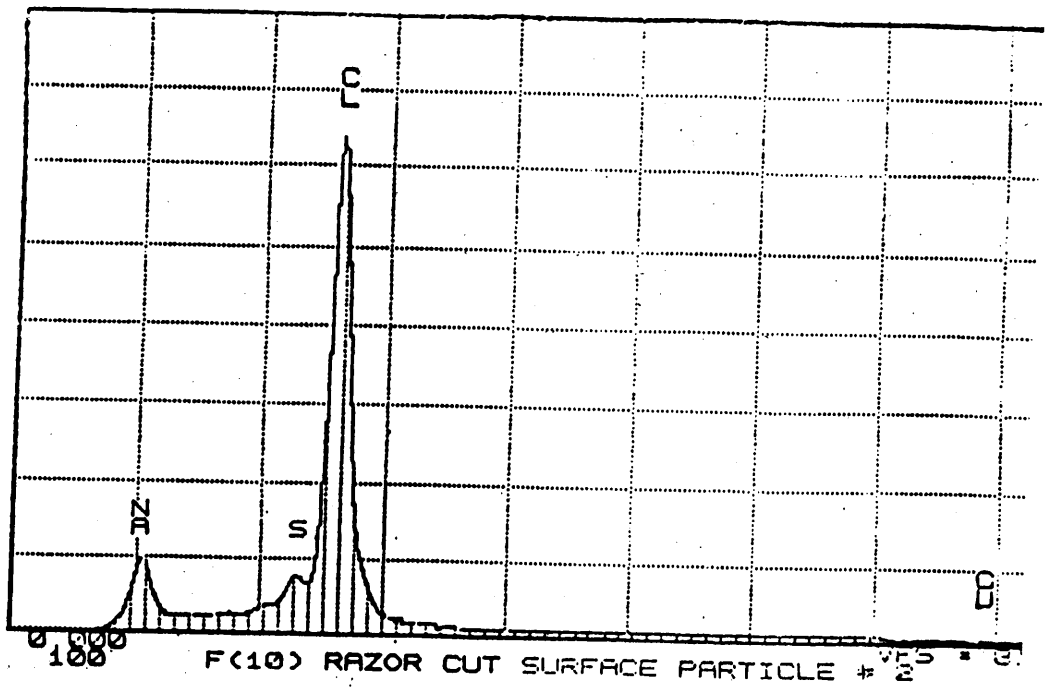

Figure 28. **EDX spectra of particulate shown in figure (27b).**

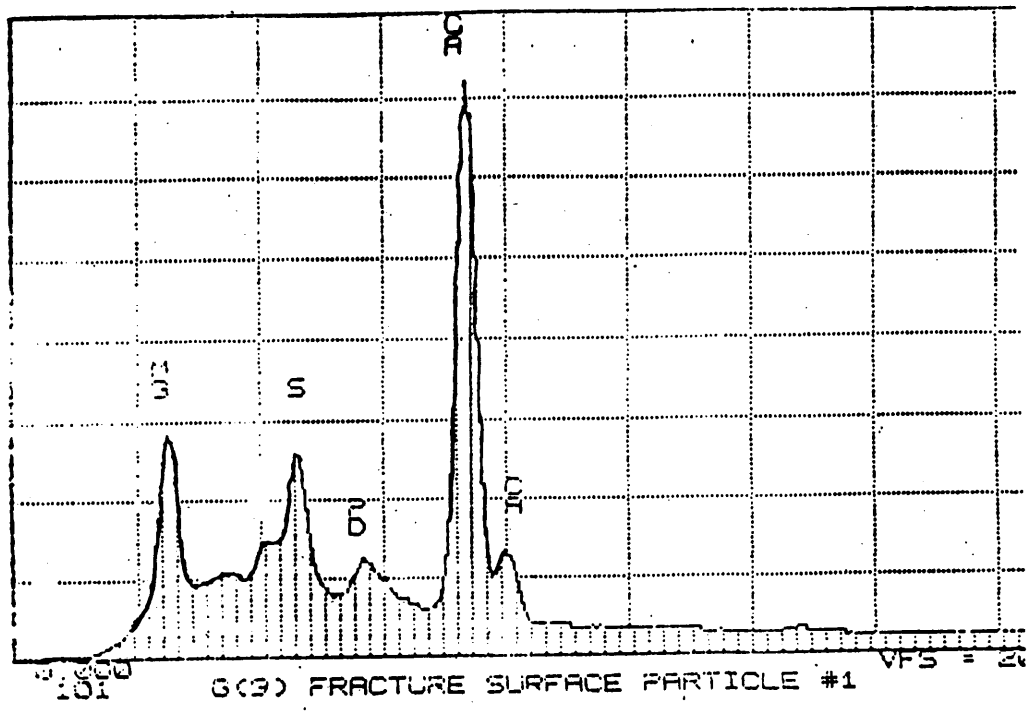

Figure 29. EDX spectra of particulate shown in figure (27c).

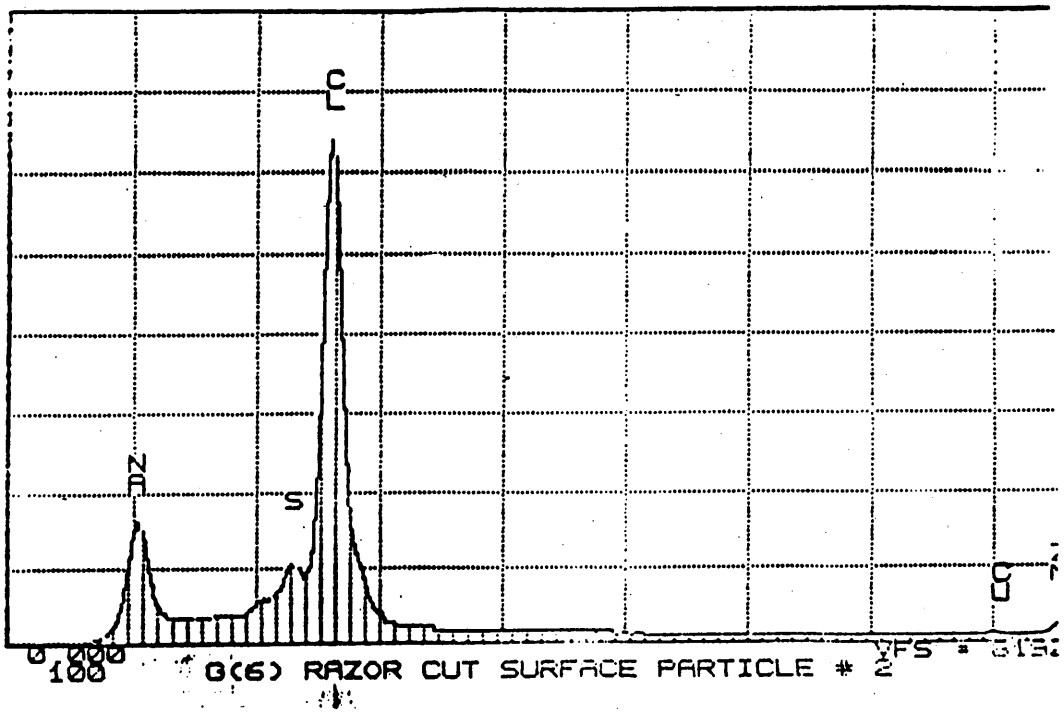

Figure 30. EDX spectra of particulate shown in figure (27d).

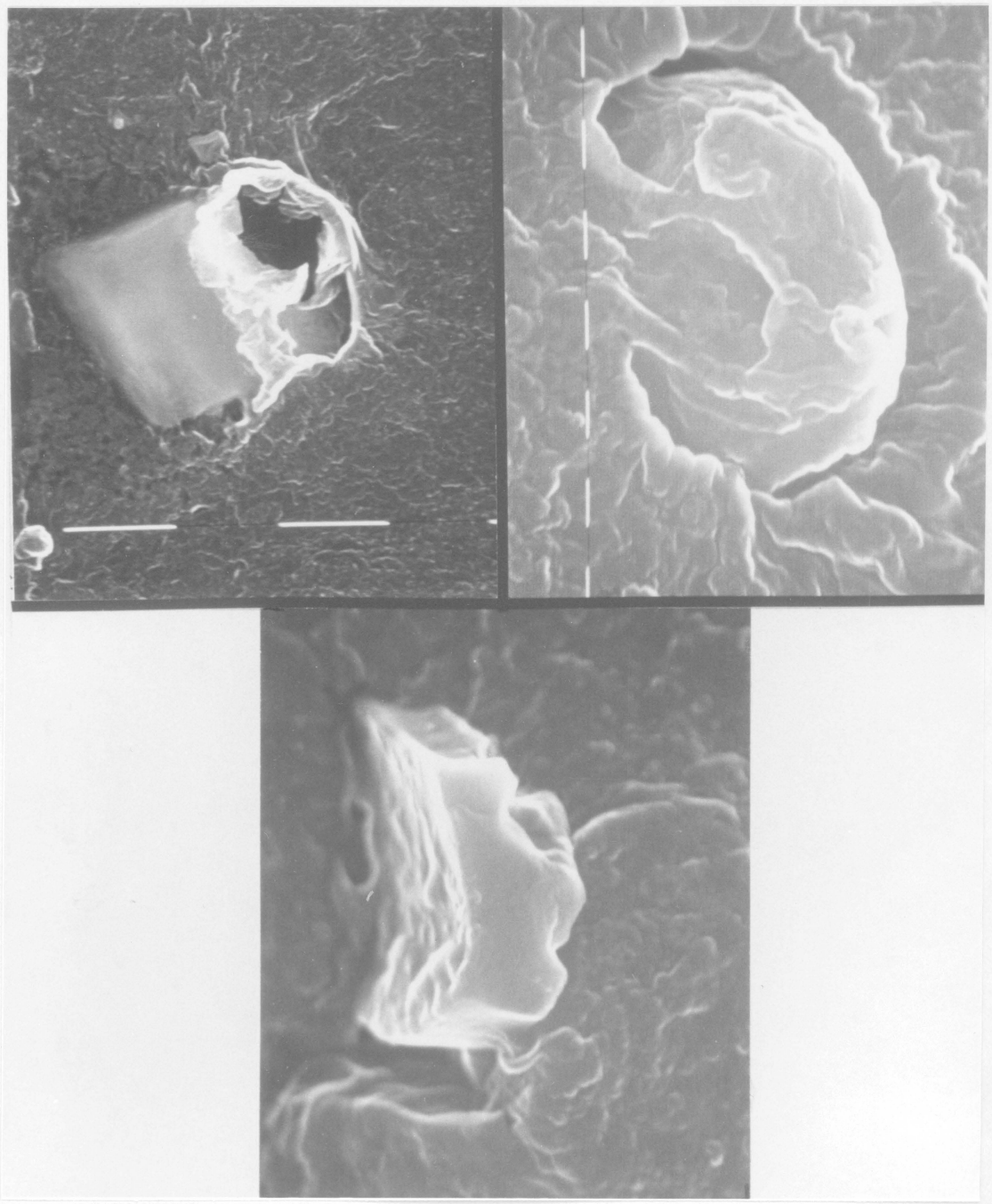

Figure 31. **Contaminants found at a razor cut surface. Sodium chloride at** a) 3200X and b) 12500X c) Sulfur at 12500X.

vulcanisation; and spread a residue around the holes. EDX identification of these holes did not reveal anything.

The origin of calcium and magnesium has been traced to the hard water used in the condensation of carbon black after removal from the furnace. Water is used to condense the fumes coming out of the furnace. If hard water is used then calcium and magnesium salts are deposited onto the black. The water finally evaporates from the surface leaving behind the calcium and magnesium. ESCA studies performed on a series of carbon blacks received from the Akron Rubber Development Labs. and Fort Belvoir showed no calcium. It is quite possible that the percentage of calcium in the black is too small to be identified by ESCA. However during the mixing process these particulates tend to concentrate in certain regions creating stress risers. The sodium chloride particles find their way into the rubber via the emulsion used in the preparation of SBR. In the preparation of SBR by emulsion polymerization, the emulsion is first created by using a surfactant. This is necessary because the monomer present in the emulsion droplets is polymerized by free radicals. After the polymerization the surfactant is to be removed. In order to do this the sodium chloride is added to the emulsion prior to coagulation. A lot of salt is left behind after the removal of the surfactant. This salt remains in the SBR after evaporation and is found on tear surfaces. Sulfur is added to facilitate crosslinking during the vulcanisation process. Some of this sulfur which is not pulverized properly prior to its introduction into the Banbury, forms a large inhomogenity as can be seen in the photomicrograph (29).

These particulates constitute inhomogenieties, cause stress concentrations and eventually give rise to sites for fracture initiation. At several points on a blowout surface were seen regions where blowout was believed to be initiated. These regions consist of a central circular region surrounded by a fine granular brittle like structure extending radially outwards in all directions as can be seen in the photomicrographs (35). The region at the centre serves as the site for 'blowout initiation' because of the presence of inhomogenities or foreign particulates, which creates stress concentration points. A synthetic fibre contaminant embedded in the rubber can be seen to have caused the blowout in the photomicrographs (36) shown below. In all the cases it can be clearly seen that the fibres were actually embedded in the rubber. The impression of the fibre in the rubber is clearly

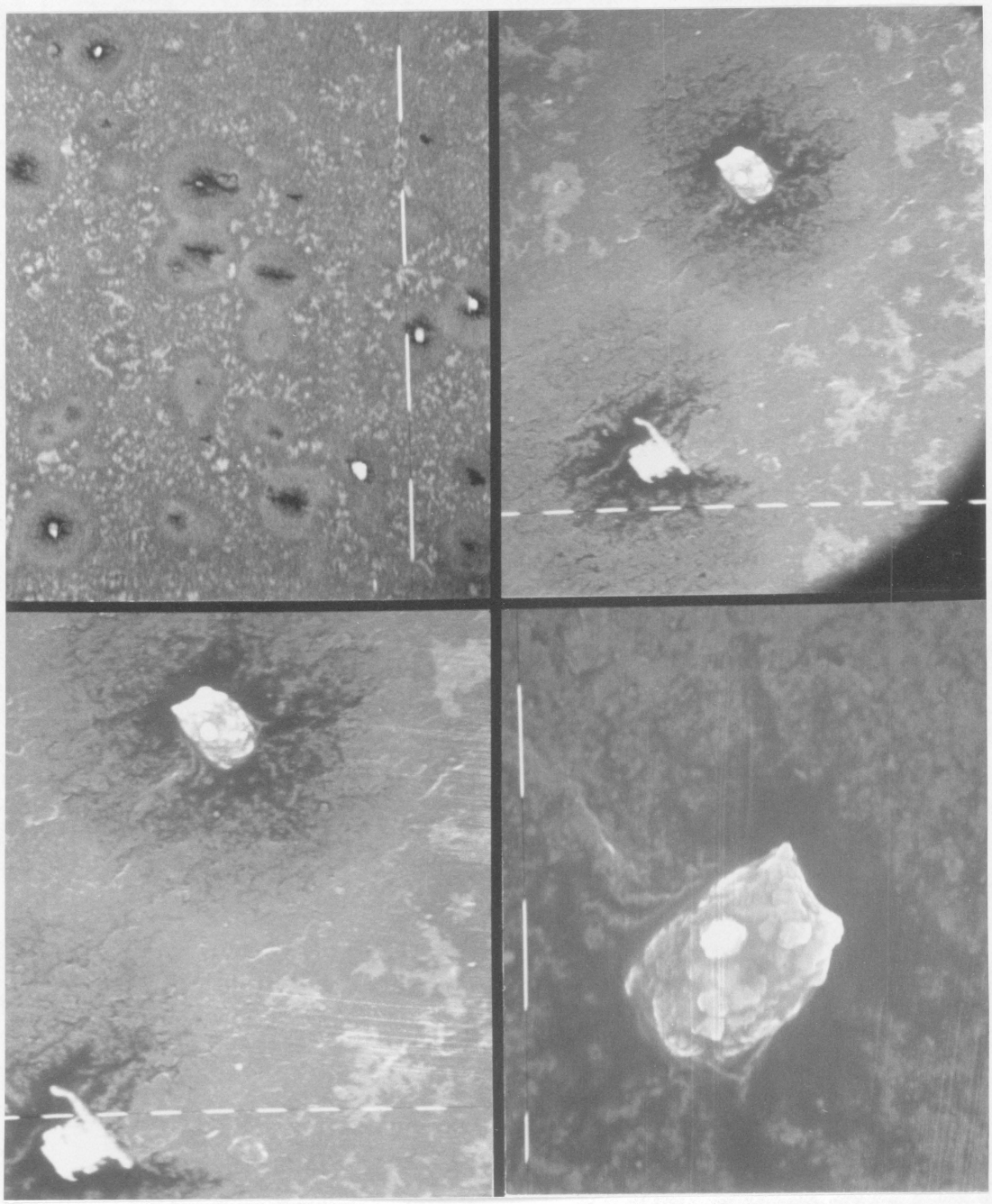

Figure 32. **Concentration of calcium at the fracture surface. a) 200X** b) 800X c)1200X d) 3200X

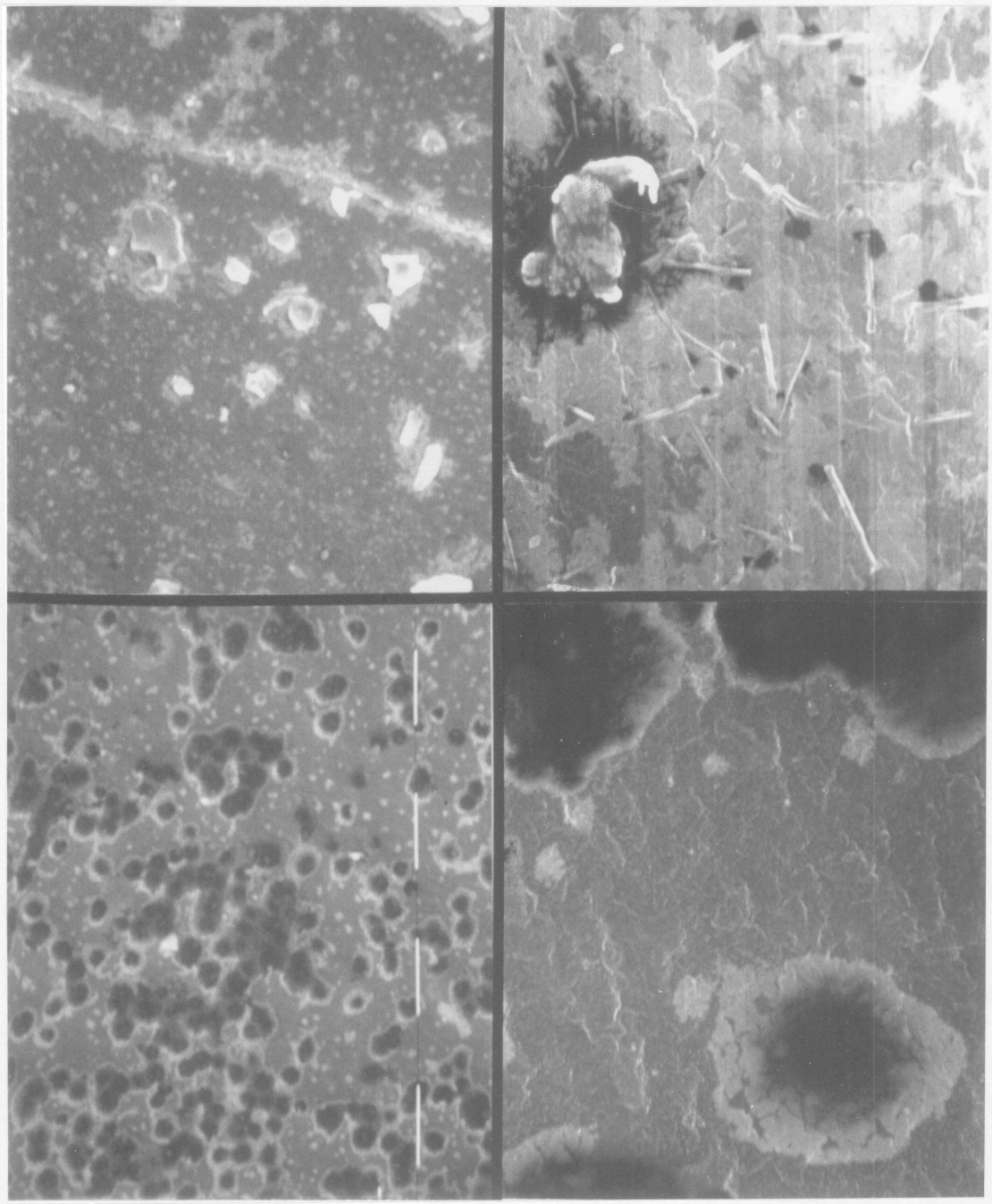

Figure 33. Distribution of contaminants on (a) and (b) Fracture surfaces. and (c) and (d) Razor cut surfaces.

visible in photographs. The content of these fibres could not determined since the EDX spectrometer cannot detect elements having atomic number below 11. In photomicrograph (36b) the flexed specimen was D-1 and had only a slight blister. The slight blister is where a blowout failure starts. It is quite obvious that the embedded fibre was responsible for causing a failure initiation site. Photomicrographs (36c) and (36d) also show sites of failure initiation where embedded fibres caused failure.

As mentioned in the earlier section on flexometer testing there are a large number of glassy regions at the blowout surfaces. Photomicrographs 37 (a), (b), (c) and (d) show a network of rectangular cracks all over the surface. The surface appears very glassy, this is due to oxidative embrittlement that takes place during flexing resulting in an increase in the crosslink density. This increase in the crosslink density, coupled with the frequency of flexing transport the Tg to a higher temperature causing the rubber to be in the glassy state. This also explains the brittle like fracture seen in the photomicrographs 38 (a), (b) and (c).

Examination in the transmission mode shows the difference in dispersion between various samples. Sections from flexed samples were cryo-ultramicrotomed at -90°C which is well below the glass transition temperature of rubber. This helps to minimise any compression lines that occur because of plastic deformation during the microsectioning. Sections were examined from specimens before and after flexing. A large number of sections from each sample were microtomed and examined using TEM. This was done in order to make a correlation between the dispersion and the measured physical and electrical properties. A visual examination of the photomicrographs shows the variations in the dispersions of carbon black agglomerates in the various samples. Sample A-2 is shown in photomicrographs (39) (a), (b) and (c); figure (a) is taken before flexing, the dispersion of black in seems almost uniform throughout. There are no agglomerates of undispersed black. Figures (b) and (c) were taken after flexing from a blowout initiation sight. Figure (b) has a uniform dispersion of black as in figure (a), however there is a large particle of zinc of approximately 0.15 micron in size. In photomicrograph (c) there seems to be a lack of dispersion as can be seen in the photomicrographed region, where there are large vacant spaces with no carbon black at all. A large agglomerate of black can be seen on the left hand side of the photomicrograph.

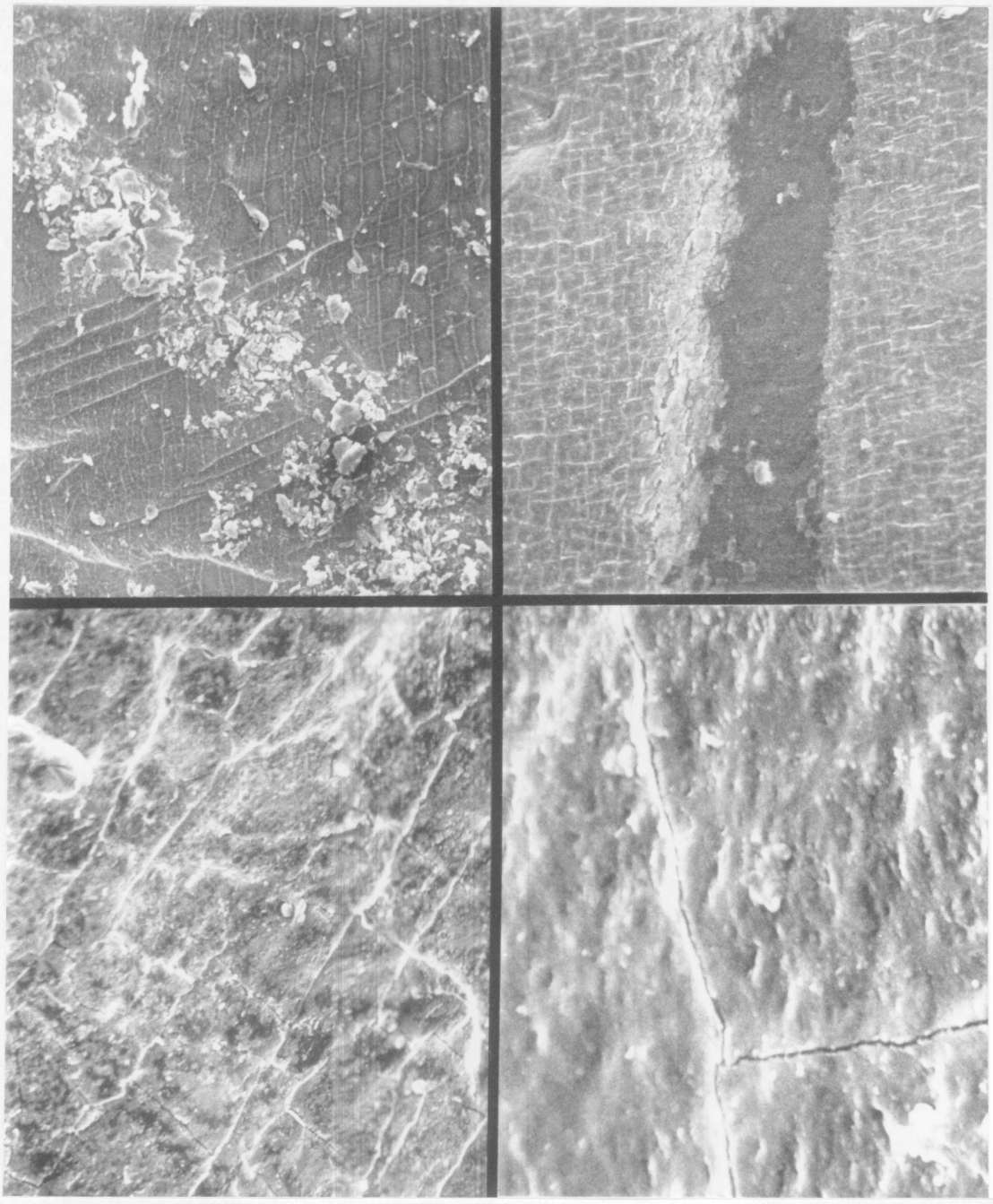

Figure 34. Glassy surface with cracks due to oxidative embrittlement.

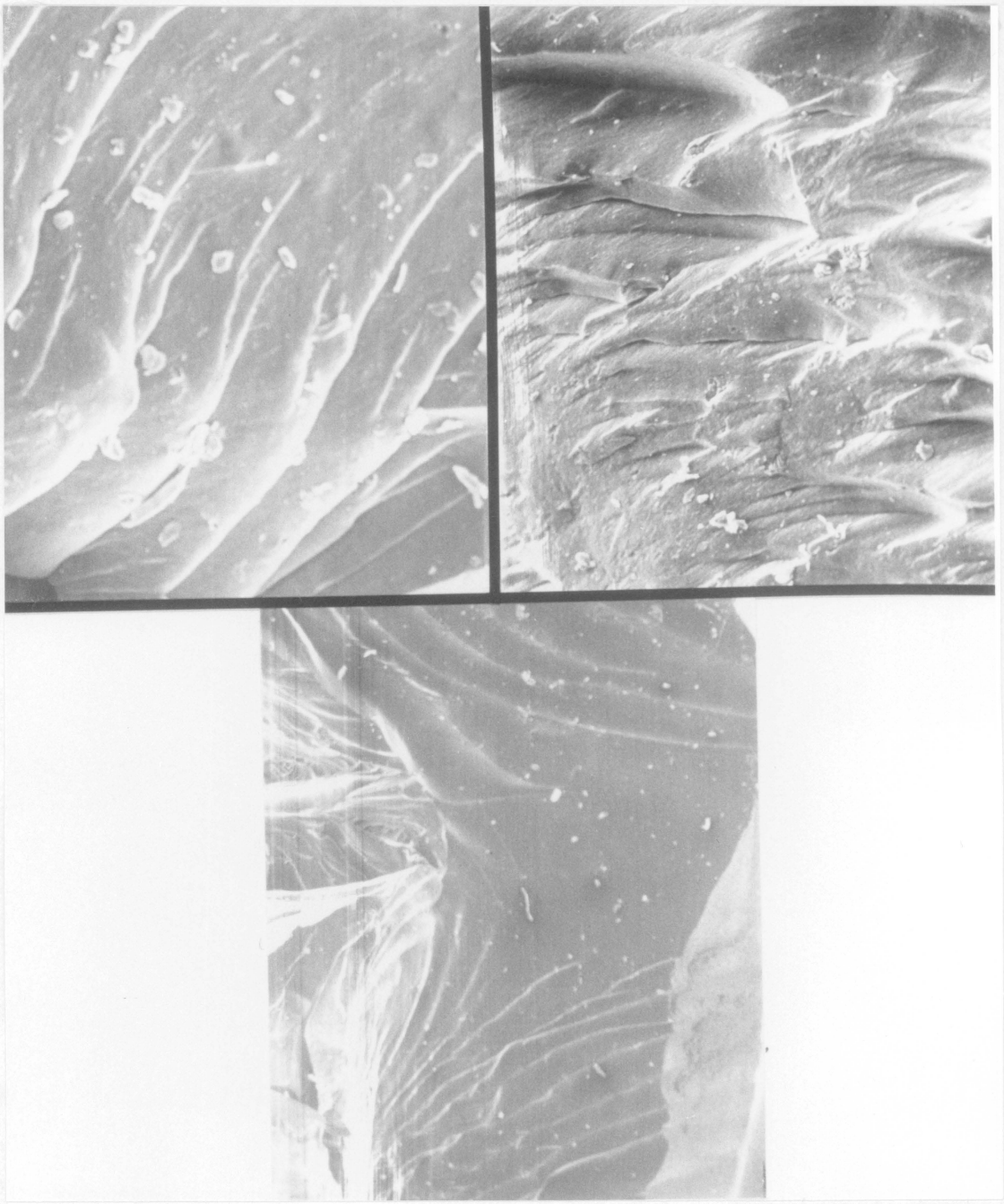

Figure 35. Brittle like fractures due to oxidative embrittlement.

A few other lumps of carbon black can be seen on the boundaries of the photomicrograph. It is debatable whether the zinc particulate or the lack of dispersion at the region, or a combination of the two factors were responsible for the blowout.

Sample A-1 was also cryo-ultramicrotomed and photographed before and after flexing. Photomicrograph (40a) which was taken from a general region before flexing shows a fairly uniform dispersion, while picture (40b) shows an unfilled region right in the centre as well several other vacant spots in the upper and lower left hand regions. The carbon- black is in the form of lumpy agglomerates which indicates that there exist certain regions where the dispersion is not of a very good quality.

Sample B-1 shows a bad dispersion both before and after flexing. This can be seen in photomicrographs (41) (a), (b) and (c). In all three photomicrographs there are large empty unfilled regions as well as regions where undispersed agglomerates are located. This can be correlated in a qualitative manner with the resistance measurements made on the sample. A very low resistance is exhibited by samples with bad dispersion. This is because these samples contain the same volume of black packed into a smaller volume of the samples, thereby increasing the number of three dimensional conductive paths available for the flow of current and hence decreasing the resistance.

Sample C-1 photomicrographs (42) (a), (b), (c) and (d) shows regions where dispersion seems to be uniform as well some where there appears to be a bad dispersion. Some agglomerates of black were seen in the microtomed samples both before and after flexing. Large zinc particulates are visible in flexed and unflexed sections. However while the unflexed section has two particulates of approximately 0.15 micron each the blowout section has one which is about 0.60 microns. Here again there does not seem to be much difference in the sections examined before and after flexing in terms of overall dispersion. The dispersion does not seem uniform as in the case of A-2 and this may explain the results obtained in the resistance measurements.

Sample D-1 shown in photomicrographs shown in figures (43) (a), (b) and (c) diplays somewhat similar dispersion characteristics as sample C-1. There are larger regions of uniform

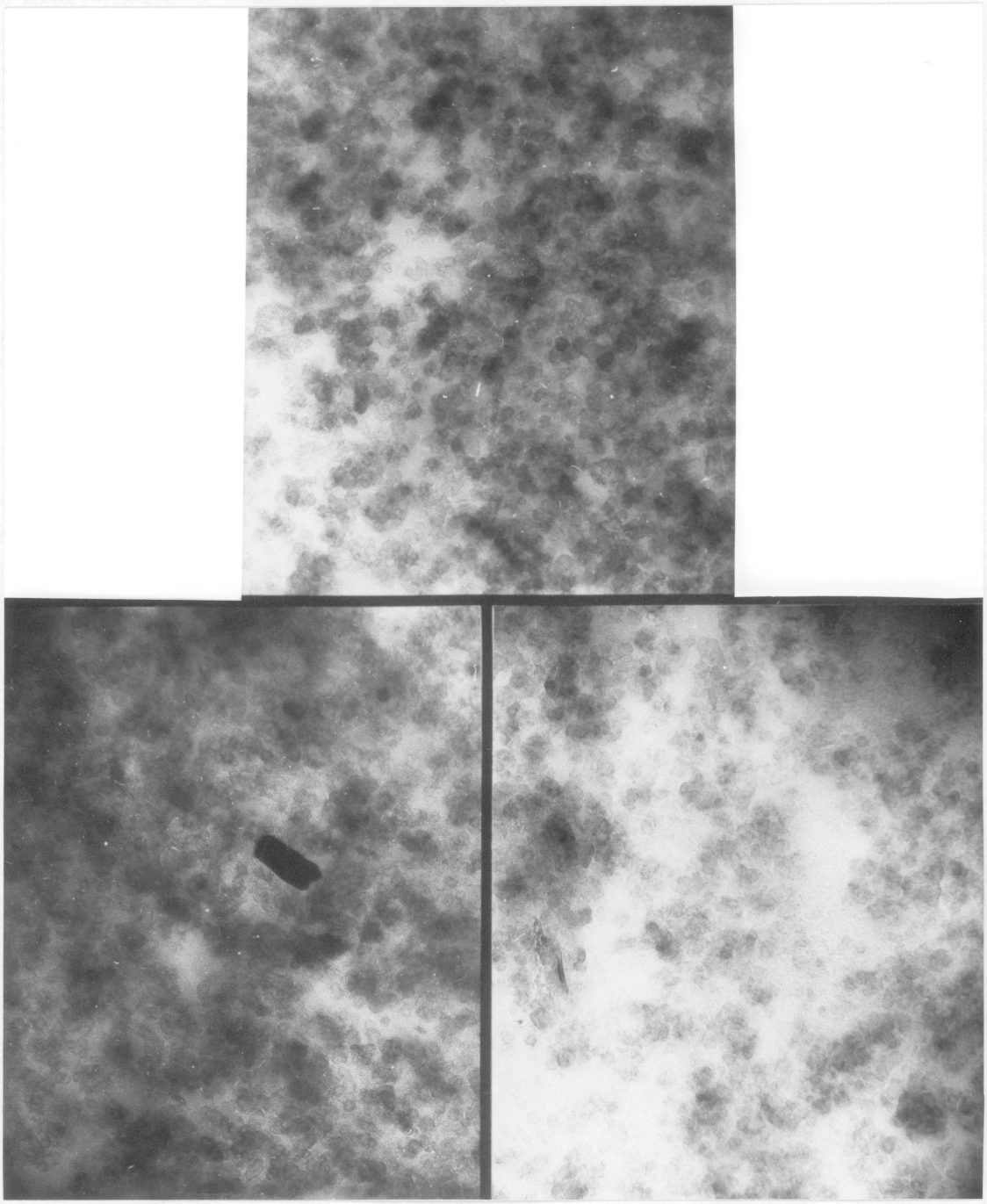

Figure 36. TEM photomicrograph of blowout section A-2. Magnification 60,000X

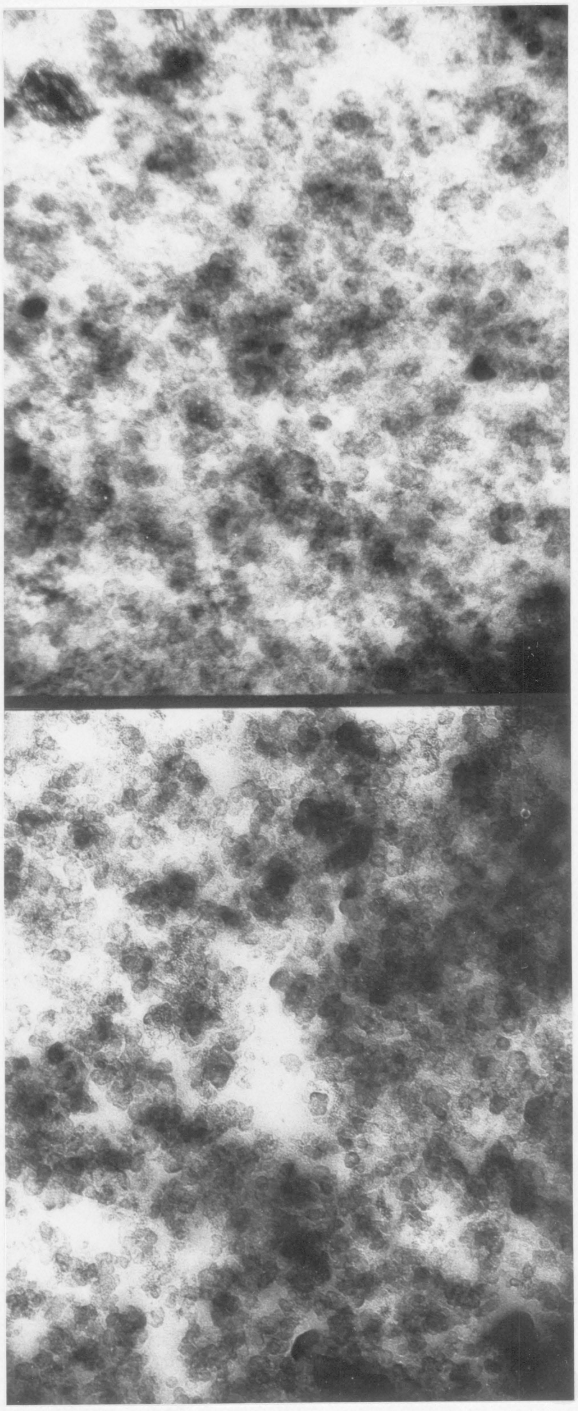

Figure 37. TEM photomicrograph of blowout section A-1. Magnification 60,000X

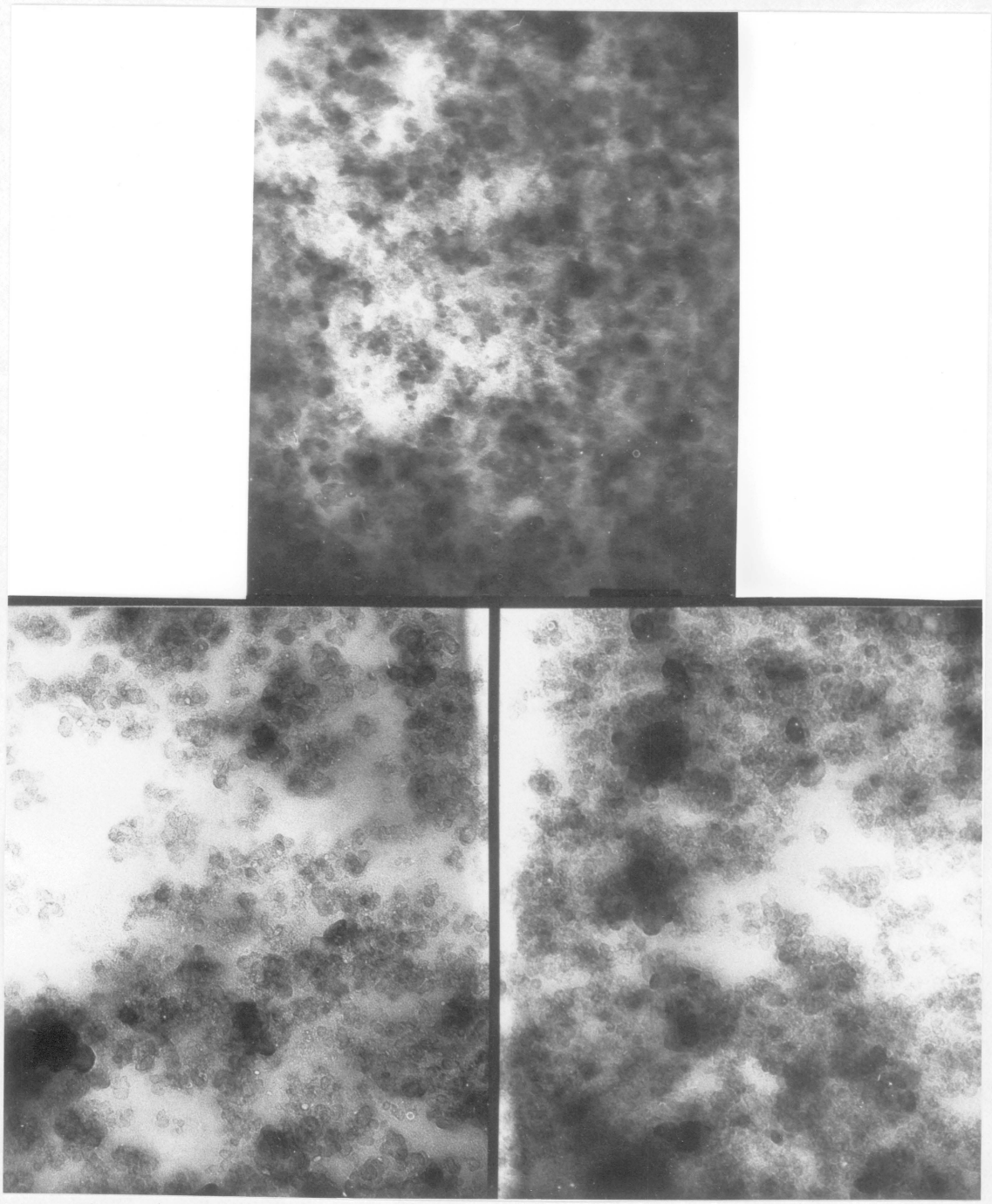

Figure 38. TEM photomicrograph of blowout section B-1. Magnification 60,000X

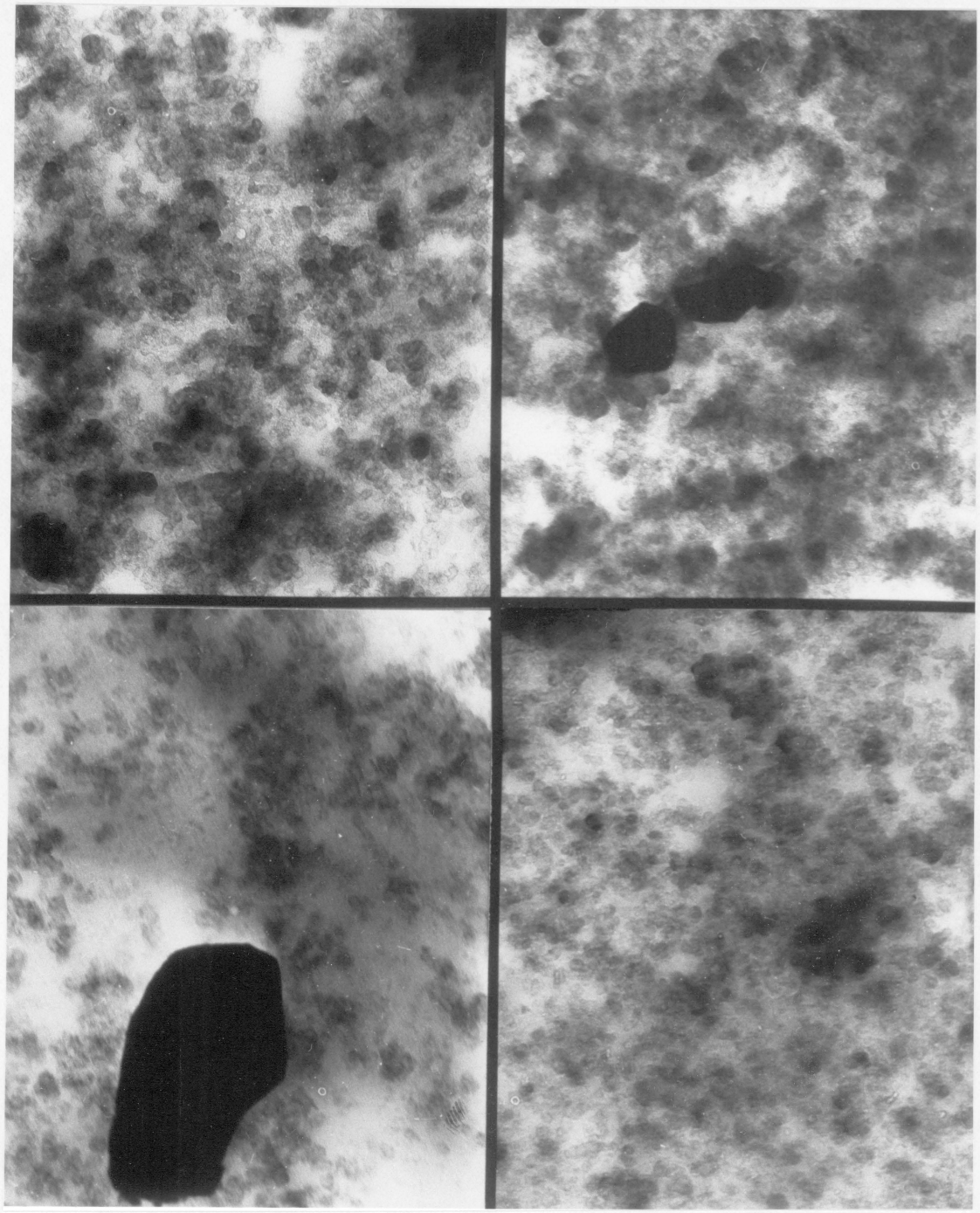

Figure 39. TEM photomicrograph of blowout section C-1. Magnification 60,000X

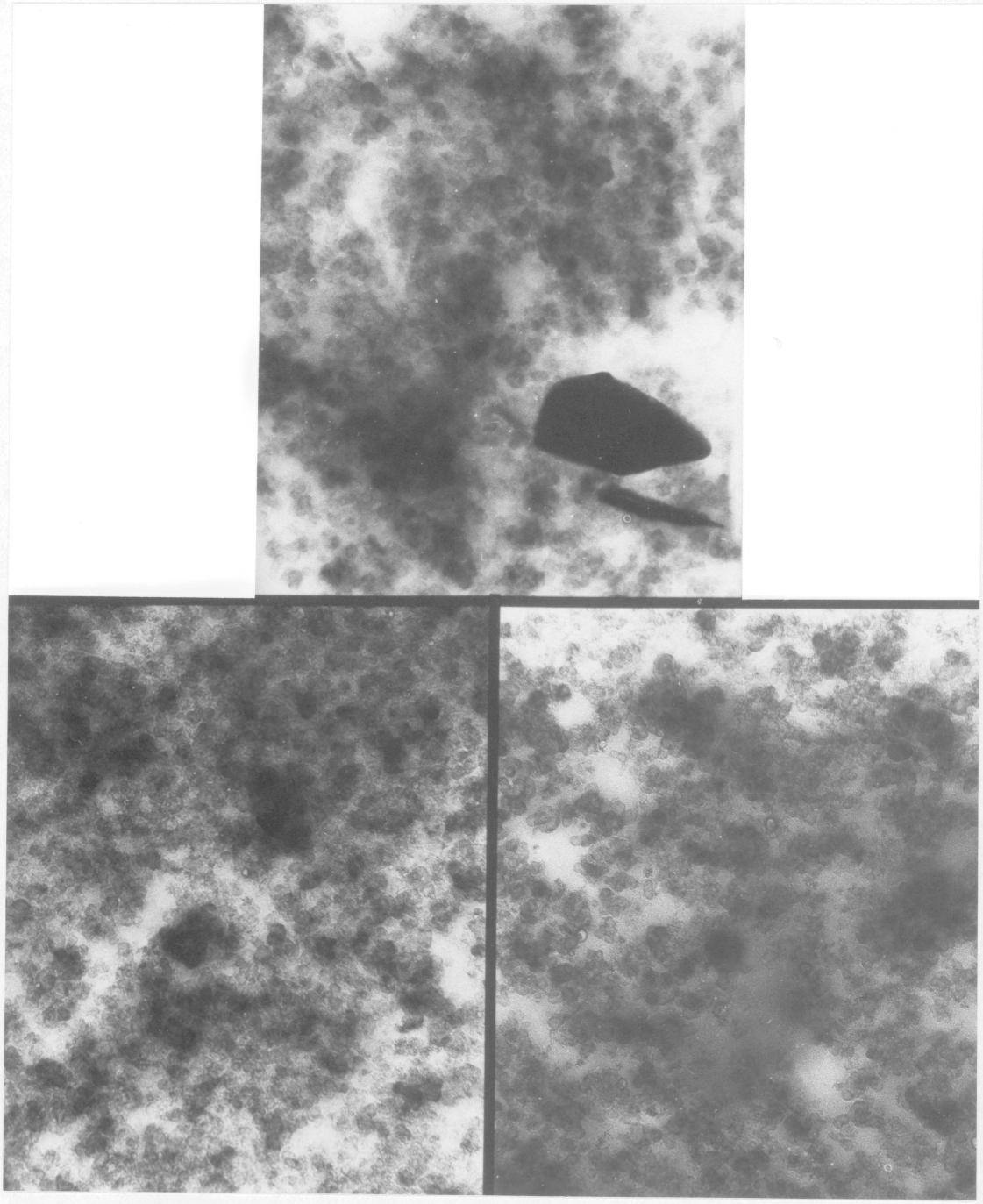

Figure 40. TEM photomicrograph of blowout section D-1. Magnification 60,000X

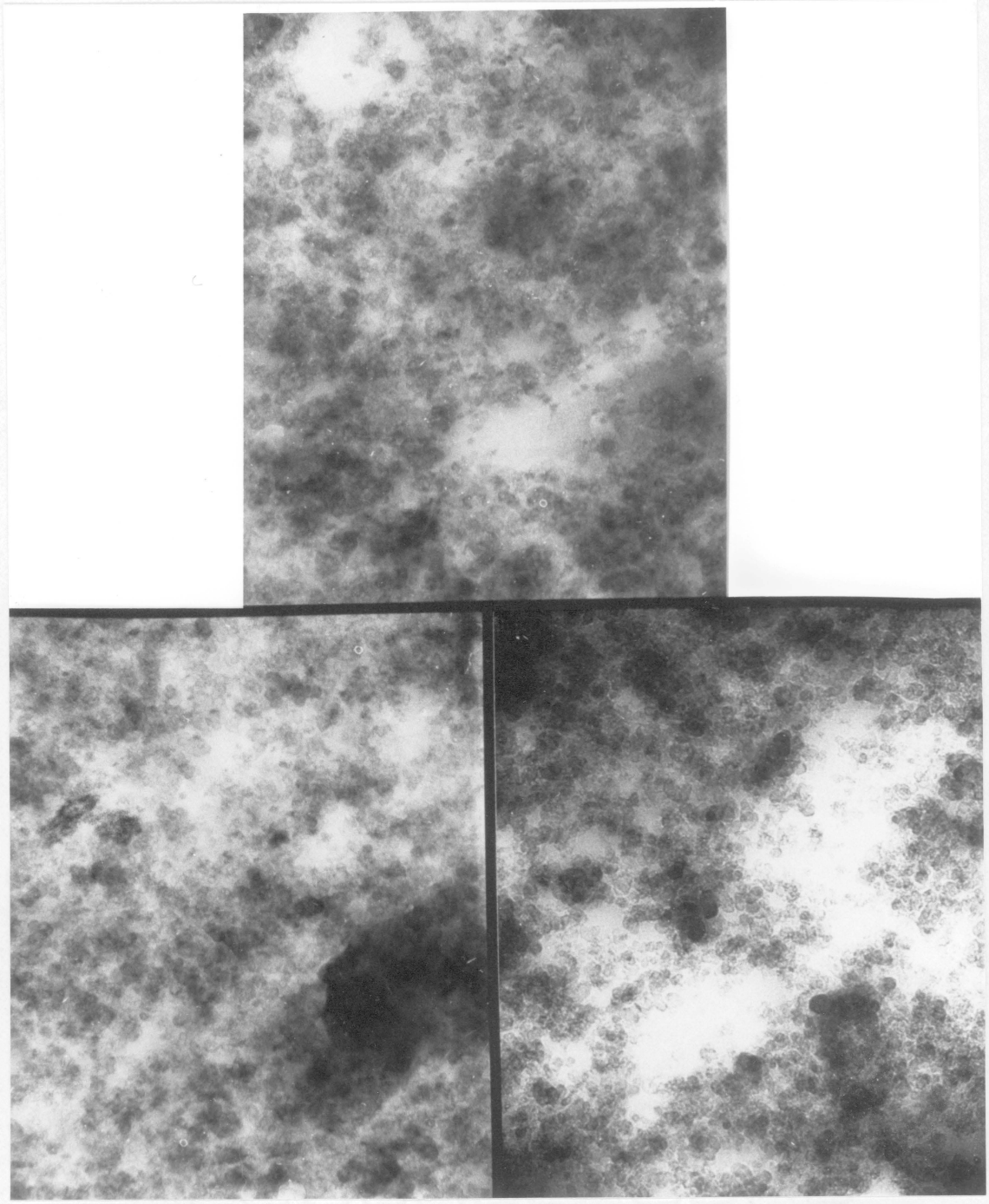

Figure 41. TEM photomicrograph of blowout section E-1. Magnification 60,000X

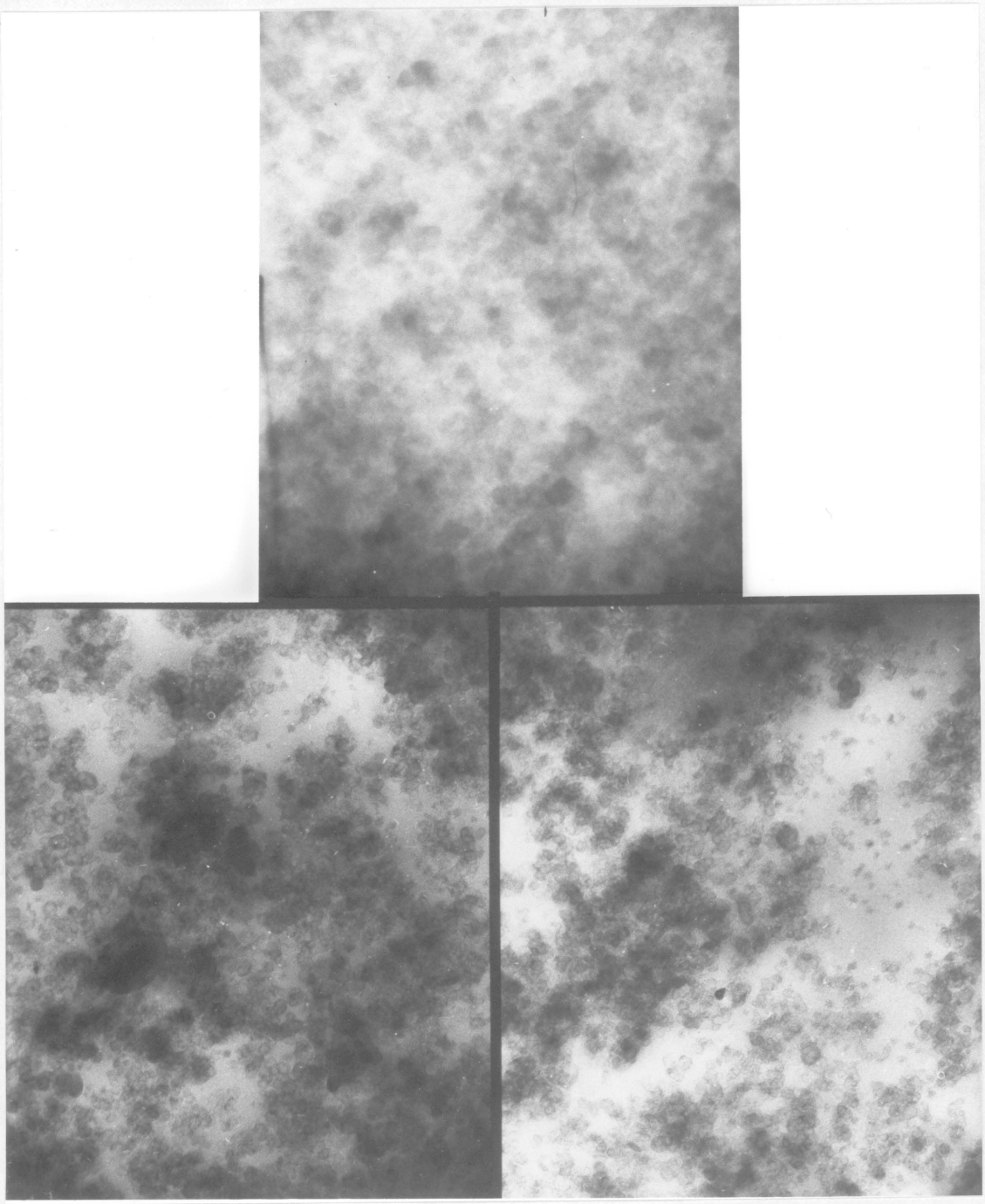

Figure 42. TEM photomicrograph of blowout section F-1. Magnification 60,000X

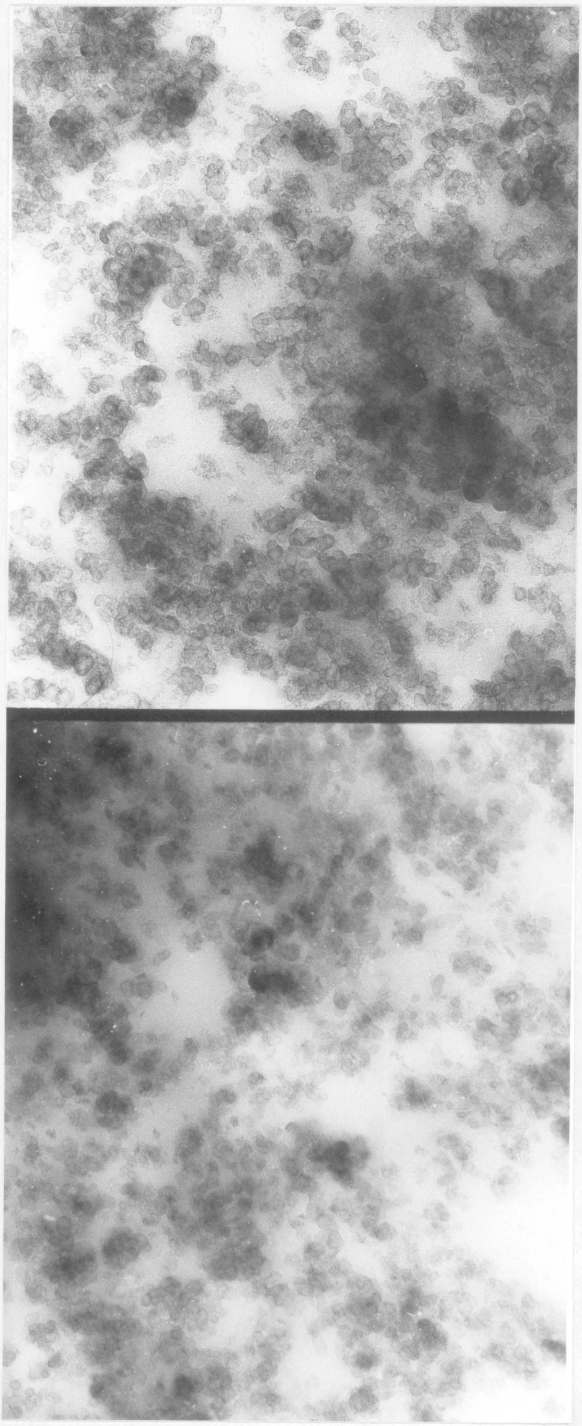

Figure 43. TEM photomicrograph of blowout section G-1. Magnification 60,000X

dispersion both before and after flexing. There are also some small regions which are unfilled in all the photomicrographs. In the photomicrograph (a) there appears some large black particles which were identified as zinc. Zinc oxide is used as a cure acceleartor in the vulcanisation. Sample shows resistance characteristics close to A-2, which indicates a good dispersion. Photomicrographs of A-2 and D-1 compare very favourably in terms of percentage areas covered by the carbon black. Hence it is difficult to see why the resistance measurements should be different. However it deserves to be pointed out that there should be a quantitative evaluation of the dispersions which can be compared with the already quantified electrical measurements.

Samples E-1, displayed in photomicrographs 44 (a), (b) and (c), sample F-1, displayed in photomicrographs 45 (a), (b) and (c), and sample G-1 displayed in photomicrographs 46 (a) and (b) have plenty in common. They are all badly dispersed showing large unfilled areas where there is not even a single black aggregate. Few other areas show lumpy undispersed agglomerates. These samples show relatively low resistances which correlate with the quality of dispersion. Sample E-1 shows a large dark patch in photomicrograph 44 (b) which was identified as a sulfur particulate.

ESCA and TEM was performed on actual tank track pad rubbers as well as the series of rubbers received from the Akron Rubber Development Laboratories. The actual tank pad rubbers were sputtered using an ion gun. Argon was used to sputter away the surface for time periods varying from 1 minute to 20 minutes. The samples were then examined on the S(T)EM using the scanning mode and secondary electron detector. Photomicrographs show that the base polymer has been degraded by the ion beam, leaving behind only carbon black and hence the surface appears to have a granular texture as can be seen in the photomicrographs. ESCA results show that sample D-1 has the highest sulfur content. This result was corroborated by the swelling tests which showed that D-1 had the highest crosslink density.

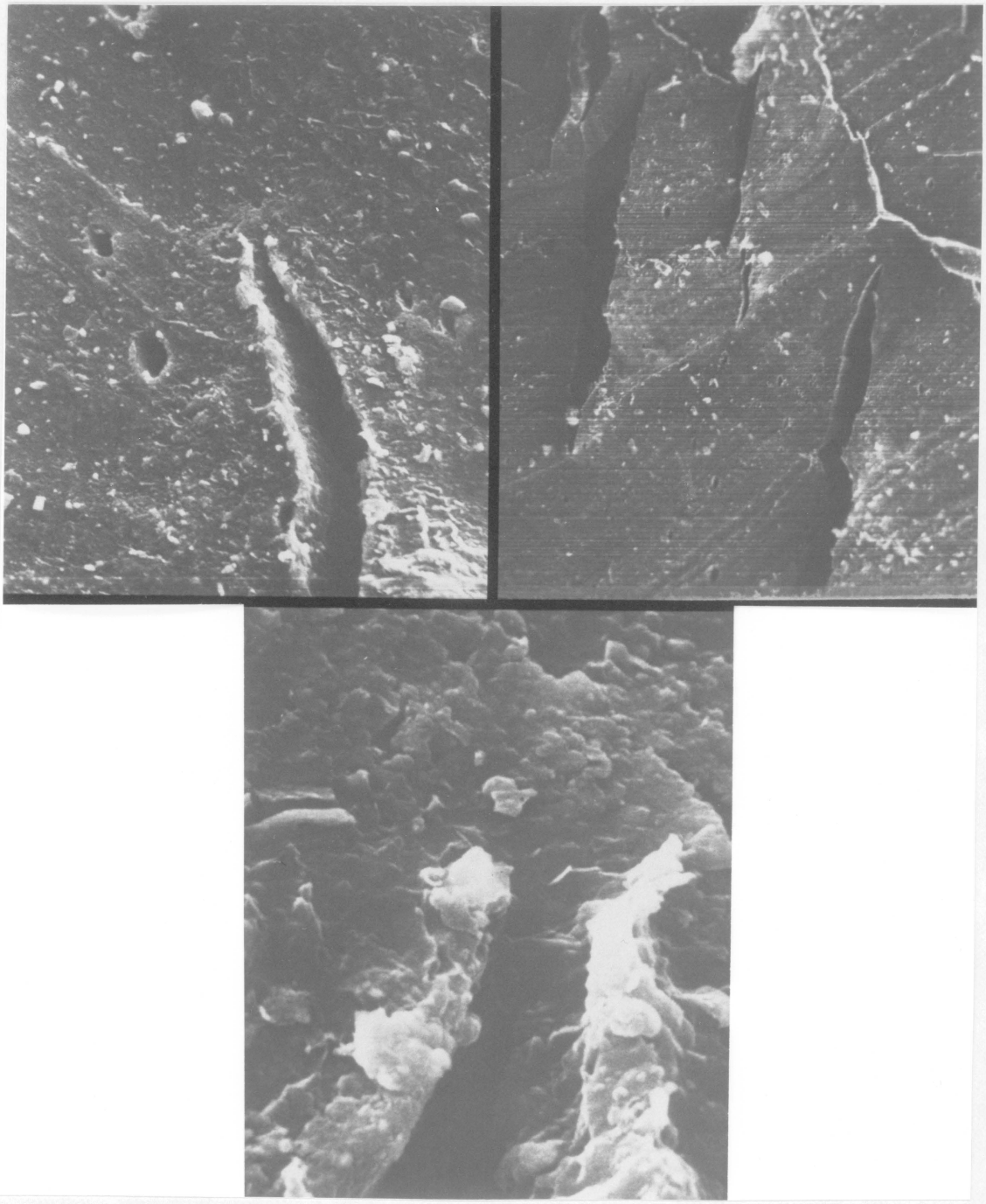

Chapter 5

5.0 SUMMARY & CONCLUSIONS

1) Variation in blending conditions produced a series of compounds with mechanical properties that changed linearly with the amount of mixing.

2) The electrical properties showed a different trend however. The samples A-2, A-1, B-1, C-1 and D-1 display resistances which appear to be parabolic when plotted against mixing time. The change in resistance on application and removal of the deforming load produces parabolic behaviour as can be seen in the histogram below (47). Samples E-1, F-1 and G-1 show linear behaviour with time of mixing.

3) A good dispersion is seen to produce a lower viscosity, a lower modulus but better tear characteristics and a lower resistance to abrasion than does a bad dispersion. In an actual track pad the resistance to abrasion as well the tear characteristics will play an important role in determining the life service of the pads mainly because these two qualities show opposing trends i. e. as abrasion resistance improves tear strength decreases and vice- versa.

4) Better dispersions produce lower moduli and consequently there is less hysteresis and a lower build up in the bulk of the rubber. This has important implications since the heat build up promotes oxidative degredation which results in the formation of voids and cracks, eventually

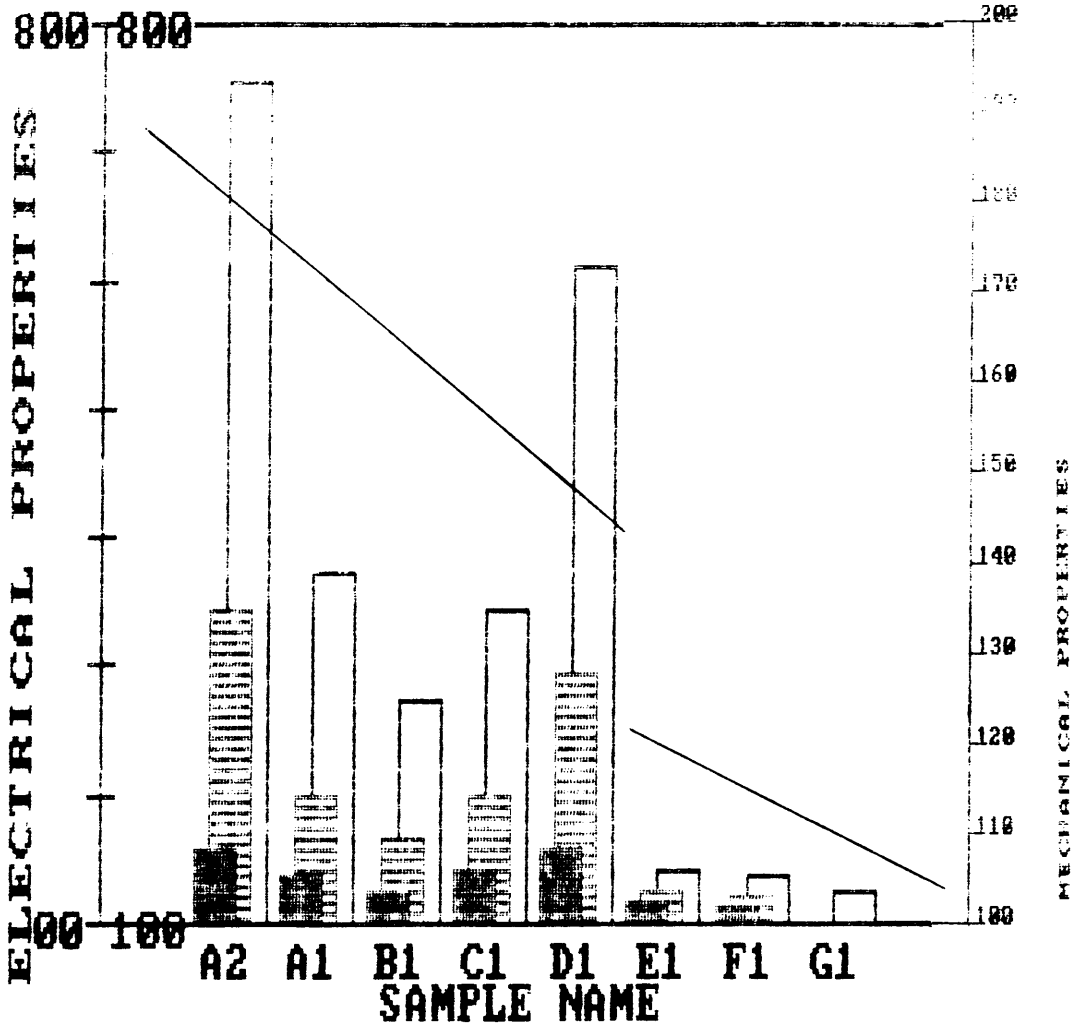

Figure 44. Histogram comparing electrical and physical properties.

leading to severe blowout. Another factor which contributes to the heat build in badly dispersed samples is stress softening.

5) The method of processing plays an important role in the characteristics of rubber compounds. Flow lines occur during processing which give rise to crack initiation and propagation. The cracks follow the flow lines. As the dispersion gets worse, flow lines become more prominent and cracks initiate much earlier and propagate much faster than in a well dispersed compound. Blowouts generally occur at the vortex of the flow lines.

6) At higher temperatures it is seen that the quality of dispersion does not play as important a role as it does at lower temperatures. This observation can be made from results obtained in the tear resistance and tensile tests. Hence the depreciatory affect on the base polymer/matrix properties by elevated temperatures cannot be compensated for by improved dispersions. Ageing of rubber products causes the modulus to increase. This is mainly due to oxidative degredation mechanisms and can have the effect of increasing the hysteresis during any cyclic processes which in turn leads to more degredation and eventually a quicker failure.

7) Inhomogenities identified by EDAX play an important role in the failure of rubber compounds. A relatively high concentration of calcium and sodium chloride particulates was seen at tear surfaces, as well as razor cut surfaces. These inhomogenities cause regions of high stress concentration and give rise to sites for failure initiation. as can be seen in figures (33). They affect physical properties in no small manner as can be seen from their concentration at failure surfaces and may be responsible for the difference in trends between electrical and physical properties.

8) The origin of the sodium chloride can be traced to the manufacturing processes of SBR i. e. sodium chloride is used to salt out the emulsion used in the preparation of SBR. Calcium finds its way into the compound because of the water used to cool the black after it is removed from the furnace. Sulfur is used as a crosslinking agent but some of it is not dispersed properly and hence it forms a large inhomogeniety.

9) The presence of inhomogenities in rubber compounds causes hot spots during the flexing which gives rise to radicals. The radicals cause scission of polymer chains. Because of the high temperatures developed, low molecular weight products volatilize and form gases, leaving behind

voids. Because of the internal pressure within the void and the non uniform strains developed during the flexing, the void develops into a crack. These crack eventually grow larger leading to catastrophic failure.

10) Phillips Dispersion Ratings are not very accurate.

Bibliography

1 E. S. Dizon, RUBBER CHEM. TECHNOL. 49, 12 (1976).

2 B. Schubert, F. P. Ford and F. Lyon " Encyclopedia of Industrial Chemical Analysis ", Vol. 8, John Wiley, New York, 1969.

3 A. I. Medalia, RUBBER CHEM. TECHNOL. 47, 411 (1974).

4 G. C. McDonald and W. M. Hess, RUBBER CHEM. TECHNOL. 50, 842 (1977).

5 A. I. Medalia, RUBBER CHEM. TECHNOL. 51, 437 (1978).

6 S. G. Main, Carbon Black Service Report; Cabot Corporation.

7 J. M. Funt, RUBBER CHEM. TECHNOL. 53, 772 (1980).

8 Z. Tadmor, Ind. Eng. Chem. Fund. 15, 346 (1976).

9 D. L. Fedyukin, T. I. Vinogradova, L. A. Danchenko and N. V. Ermilova RUBBER CHEM. TECHNOL. 46, 511 (1973).

10 G. Kraus, RUBBER CHEM. TECHNOL. 44, 199 (1971).

11 G. R. Cotton, RUBBER CHEM. TECHNOL. 58, 774 (1985).

12 J. M. Funt "Rubber Mixing" RAPRA PUBLICATION, Showburg, U. K., 1977.

13 Rigby Zvi, Advances in Polymer Sci. 36,21-68 (1980).

14 Jay Jansen and Gerard Kraus, RUBBER CHEM. TECHNOL. 53,48 (1980).

15 P. C. Ebell and D. A. Hemsley, RUBBER CHEM. TECHNOL. 54, 698 (1981).

16 R. W. Sambrook, Journal of the IRI 4, 210-6 (1970).

17 Sin-Shong LIN, Applied Surface Science 26 (1986) 461-471.

18 N. M. Mathew, A. K. Bhowmick and S. K. De, RUBBER CHEM. TECHNOL. 55, 51 (1982).

19 S. K. Chakraborthy, A. K. Bhowmick, S.K. De and B. K. Dhindaw, RUBBER CHEM. TECHNOL 55, 41 (1986).

20 A. G. Thomas, J. Polym. Sci. 145

21 A. N. Gent, P. B. Lidley, and A. G. Thomas, J. Appl. Polym. Sci. 8, 455 (1964).

22 A. G. Thomas, Physical Basis of Yield and Fracture, Conference Proceedings, Oxford, 1966, p. 134.

23 A. R. Payne, J. Appl. Polym. Sci., 6, 57 (1962).

24 A. R. Payne, J. Appl. Polym. Sci., 7, 873 (1963).

25 A. R. Payne, J. Appl. Polym. Sci., 8, 2661 (1964).

26 A. R. Payne, J. Appl. Polym. Sci., 9, 2273 (1965).

27 A. R. Payne, J. Appl. Polym. Sci.,

28 E. M. Dannenberg, Trans. IRI, 42, T26 (1966).

29 P. C. Vegvari, W. M. Hess, and V. E. Chiroco, RUBBER CHEM. TECHNOL. 51, 817 (1978).

30 N. A. Stumpe Jr. and H. E. Railsback, Rubber World 151(3), 41 (1964).

31 C. H. Leigh-Dugmore, RUBBER CHEM. TECHNOL. 29, 1303 (1956).

32 R. J. Cembrola, RUBBER CHEM. TECHNOL. 56, 233 (1983).

33 A. I. Medalia, RUBBER CHEM. TECHNOL. 59,434 (1986).

34 Norman R. H. 'Conductive Rubbers and Plastics', Elsevier, London, (1970).

35 B. B. S. T. Boonstra and A. I. Medalia, RUBBER CHEM. TECHNOL. 36, 115 (1963).

36 C. W. Sweitzer, W. M. Hess and J. E. Callan, Rubber World 167(2), 147 (1972).

37 W. C. Schneider, W. C. Carter, M. Magat, and C. P. Smythe, Amer. Chem. Soc, 67(1), 959 (1945).

38 J. I. Goldstein and H. Yakowitz, Practical Scanning Electron Microscopy, Plenum, 1976.

39 Kevex Corporation, An Introduction to Energy Dispersive Microanalysis (1983).

40 Handbook of Photoelectron Spectroscopy, Perkin-Elmer (1979).

41 N. H. Lawrence, Thesis, VPI&SU, (1984).

The vita has been removed from the scanned document